UNITED STATES

DEPARTMENT OF THE INTERIOR

U.S. GEOLOGICAL SURVEY

ESTIMATION OF RESPONSE SPECTRA AND PEAK ACCELERATIONS FROM WESTERN NORTH AMERICAN EARTHQUAKES: AN INTERIM REPORT

PART 2

David M. Boore, William B. Joyner, and Thomas E. Fumal

U.S. GEOLOGICAL SURVEY OPEN-FILE REPORT 94-127

Menlo Park, California

1994

****

These initial pages were prepared after publication of Open-File Report 94–127 and are bound in here for the convenience of the reader.

****

GROUND MOTION ESTIMATES FOR STRIKE- AND REVERSE-SLIP FAULTS

David M. Boore
William B. Joyner
Thomas E. Fumal

In our previous work (Boore, Joyner, and Fumal, 1993; hereafter referred to as 'BJF93') we presented equations for ground-motion prediction in which we did not differentiate between the style of faulting. Subsequent to BJF93 we published a report in which we showed that there is a discernable difference between ground motions from strike-slip and reverse-slip earthquakes (figure 8 in Boore, Joyner, and Fumal, 1994; hereafter referred to as 'BJF94'). The purpose of this note is to present equations for ground-motion prediction that include the effect of fault type.

We classified earthquakes into strike-slip and reverse-slip classes according to the rake angle (within 30 degrees of horizontal for strike slip); the assignments are given in Table 5 of BJF94. We used the following equation for ground motion:

$$\log Y = b_{SS}G_{SS} + b_{RS}G_{RS} + b_2(\mathbf{M}-6) + b_3(\mathbf{M}-6)^2 + b_4 r + b_5 \log r + b_6 G_B + b_7 G_C$$

where

$$r = (d^2 + h^2)^{(1/2)}$$

and G_{SS} and G_{RS} take values of 1.0 for strike-slip and reverse-slip earthquakes, respectively, and 0.0 otherwise. This equation is identical to equation (1) in BJF93 except that the term b_1 in BJF93 has been replaced by the terms involving b_{SS} and b_{RS}. We assumed the same coefficients for b_2 through b_7 as found in BJF93 and solved for b_{SS} and b_{RS}; the results are given in the attached tables (please note that the column heading 'B1RV' should be 'B1RS' and that coefficients have not been provided for the larger of the horizontal components or for dampings other than 5 percent). The definitions of the predictor variables are given in BJF93, as is the meaning of the uncertainties in the last three columns. The total uncertainty has not been given in the tables; it can be computed from the equation:

$$\sigma_{\log Y} = (SIG1^2 + SIGE^2 + SIGC^2)^{(1/2)}.$$

REFERENCES

Boore, David M., William B. Joyner, and Thomas E. Fumal (1993). Estimation of response spectra and peak accelerations from western North American earthquakes: An interim report, *U. S. Geol. Surv. Open-File Rept. 93-509*, 72 pp.

Boore, David M., William B. Joyner, and Thomas E. Fumal (1994). Estimation of response spectra and peak accelerations from western North American earthquakes: An interim report, Part 2, *U. S. Geol. Surv. Open-File Rept. 94-127*, 40 pp.

COEFFICIENTS FOR CALCULATING RESPONSE SPECTRA AT 5 PERCENT DAMPING FOR THE RANDOM HORIZONTAL COMPONENT

D. M. BOORE, W. B. JOYNER, AND T. E. FUMAL

(SEE U.S. GEOLOGICAL SURVEY OPEN-FILE REPORT 93-509)

LOGPER	PER	B1SS	B1RV	B1ALL	B2	B3	H	B4	B5	B6	B7	B8	SIG1	SIGE	SIGC
-1.000	0.100	1.630	1.665	1.653	0.327	-0.098	6.27	0.00000	-0.934	0.046	0.136	0.000	0.191	0.000	0.082
-0.959	0.110	1.700	1.740	1.725	0.318	-0.100	6.65	0.00000	-0.937	0.071	0.156	0.000	0.190	0.000	0.087
-0.921	0.120	1.754	1.800	1.782	0.313	-0.101	6.91	0.00000	-0.939	0.093	0.174	0.000	0.190	0.000	0.091
-0.886	0.130	1.797	1.848	1.828	0.309	-0.101	7.08	0.00000	-0.939	0.111	0.191	0.000	0.189	0.000	0.094
-0.854	0.140	1.832	1.887	1.864	0.307	-0.100	7.18	0.00000	-0.938	0.127	0.206	0.000	0.189	0.000	0.097
-0.824	0.150	1.859	1.918	1.892	0.305	-0.099	7.23	0.00000	-0.937	0.140	0.221	0.000	0.189	0.000	0.100
-0.796	0.160	1.880	1.943	1.915	0.305	-0.098	7.24	0.00000	-0.935	0.153	0.234	0.000	0.189	0.000	0.102
-0.770	0.170	1.897	1.963	1.933	0.305	-0.096	7.21	0.00000	-0.933	0.163	0.246	0.000	0.189	0.000	0.104
-0.745	0.180	1.910	1.979	1.948	0.306	-0.094	7.16	0.00000	-0.930	0.173	0.258	0.000	0.189	0.001	0.106
-0.721	0.190	1.920	1.992	1.959	0.308	-0.092	7.10	0.00000	-0.927	0.182	0.269	0.000	0.189	0.002	0.108
-0.699	0.200	1.928	2.002	1.967	0.309	-0.090	7.02	0.00000	-0.924	0.190	0.279	0.000	0.189	0.004	0.109
-0.658	0.220	1.937	2.015	1.978	0.313	-0.086	6.83	0.00000	-0.918	0.203	0.297	0.000	0.190	0.007	0.112
-0.620	0.240	1.941	2.022	1.982	0.318	-0.082	6.62	0.00000	-0.912	0.214	0.314	0.000	0.190	0.011	0.114
-0.585	0.260	1.940	2.024	1.982	0.323	-0.078	6.39	0.00000	-0.906	0.224	0.329	0.000	0.190	0.014	0.116
-0.553	0.280	1.936	2.023	1.979	0.329	-0.073	6.17	0.00000	-0.899	0.232	0.343	0.000	0.191	0.017	0.118
-0.523	0.300	1.930	2.019	1.974	0.334	-0.070	5.94	0.00000	-0.893	0.239	0.356	0.000	0.191	0.021	0.120
-0.495	0.320	1.923	2.013	1.967	0.340	-0.066	5.72	0.00000	-0.888	0.245	0.367	0.000	0.192	0.024	0.121
-0.469	0.340	1.915	2.006	1.959	0.345	-0.062	5.50	0.00000	-0.882	0.251	0.378	0.000	0.193	0.028	0.122
-0.444	0.360	1.906	1.997	1.950	0.350	-0.059	5.30	0.00000	-0.877	0.256	0.387	0.000	0.193	0.031	0.123
-0.420	0.380	1.897	1.988	1.940	0.356	-0.055	5.10	0.00000	-0.872	0.260	0.396	0.000	0.194	0.034	0.124
-0.398	0.400	1.887	1.979	1.930	0.361	-0.052	4.91	0.00000	-0.867	0.264	0.405	0.000	0.194	0.037	0.125
-0.377	0.420	1.877	1.969	1.920	0.365	-0.049	4.74	0.00000	-0.862	0.267	0.413	0.000	0.195	0.040	0.126
-0.357	0.440	1.868	1.959	1.910	0.370	-0.047	4.57	0.00000	-0.858	0.271	0.420	0.000	0.195	0.043	0.127
-0.337	0.460	1.858	1.950	1.900	0.375	-0.044	4.41	0.00000	-0.854	0.273	0.427	0.000	0.196	0.045	0.128
-0.319	0.480	1.849	1.940	1.890	0.379	-0.042	4.26	0.00000	-0.850	0.276	0.433	0.000	0.196	0.048	0.129
-0.301	0.500	1.839	1.930	1.881	0.384	-0.039	4.13	0.00000	-0.846	0.279	0.439	0.000	0.197	0.050	0.130
-0.260	0.550	1.817	1.906	1.857	0.394	-0.034	3.82	0.00000	-0.837	0.284	0.452	0.000	0.198	0.056	0.131
-0.222	0.600	1.797	1.883	1.835	0.403	-0.030	3.57	0.00000	-0.830	0.289	0.464	0.000	0.199	0.062	0.133
-0.187	0.650	1.779	1.862	1.815	0.411	-0.026	3.36	0.00000	-0.823	0.293	0.474	0.000	0.200	0.067	0.134
-0.155	0.700	1.763	1.842	1.797	0.418	-0.023	3.20	0.00000	-0.818	0.297	0.483	0.000	0.201	0.072	0.135
-0.125	0.750	1.748	1.824	1.781	0.425	-0.020	3.07	0.00000	-0.813	0.300	0.490	0.000	0.202	0.076	0.136
-0.097	0.800	1.736	1.807	1.766	0.431	-0.018	2.98	0.00000	-0.809	0.303	0.497	0.000	0.203	0.080	0.137
-0.071	0.850	1.725	1.792	1.753	0.437	-0.016	2.92	0.00000	-0.805	0.306	0.503	0.000	0.203	0.083	0.139
-0.046	0.900	1.716	1.779	1.742	0.442	-0.015	2.89	0.00000	-0.802	0.309	0.508	0.000	0.204	0.087	0.140
-0.022	0.950	1.708	1.766	1.732	0.446	-0.014	2.88	0.00000	-0.800	0.312	0.513	0.000	0.205	0.090	0.141
0.000	1.000	1.701	1.755	1.724	0.450	-0.014	2.90	0.00000	-0.798	0.314	0.517	0.000	0.206	0.093	0.141
0.041	1.100	1.692	1.737	1.710	0.457	-0.013	2.99	0.00000	-0.795	0.319	0.523	0.000	0.207	0.098	0.143
0.079	1.200	1.688	1.723	1.701	0.462	-0.014	3.14	0.00000	-0.794	0.324	0.528	0.000	0.208	0.102	0.145
0.114	1.300	1.687	1.712	1.696	0.466	-0.015	3.36	0.00000	-0.793	0.328	0.532	0.000	0.209	0.106	0.147
0.146	1.400	1.690	1.705	1.695	0.469	-0.017	3.62	0.00000	-0.794	0.333	0.535	0.000	0.210	0.109	0.148
0.176	1.500	1.695	1.701	1.696	0.471	-0.019	3.92	0.00000	-0.796	0.338	0.537	0.000	0.211	0.111	0.150
0.204	1.600	1.703	1.699	1.700	0.472	-0.022	4.26	0.00000	-0.798	0.342	0.538	0.000	0.212	0.114	0.151
0.230	1.700	1.714	1.699	1.706	0.473	-0.025	4.62	0.00000	-0.801	0.347	0.539	0.000	0.213	0.116	0.153
0.255	1.800	1.726	1.702	1.715	0.472	-0.029	5.01	0.00000	-0.804	0.351	0.539	0.000	0.214	0.117	0.154
0.279	1.900	1.740	1.706	1.725	0.472	-0.032	5.42	0.00000	-0.808	0.356	0.538	0.000	0.214	0.119	0.156
0.301	2.000	1.756	1.712	1.737	0.471	-0.037	5.85	0.00000	-0.812	0.360	0.537	0.000	0.215	0.120	0.157

COEFFICIENTS FOR CALCULATING PEAK ACCELERATION FOR THE RANDOM HORIZONTAL COMPONENT
D. M. BOORE, W. B. JOYNER, AND T. E. FUMAL
(SEE U.S. GEOLOGICAL SURVEY OPEN-FILE REPORT 93-509)

B1SS	BIRV	B1ALL	B2	B3	H	B4	B5	B6	B7	B8	SIG1	SIGE	SIGC
-0.136	-0.051	-0.105	0.229	0.000	5.57	0.00000	-0.778	0.162	0.251	0.000	0.187	0.080	0.098

COEFFICIENTS FOR CALCULATING PEAK ACCELERATION FOR THE LARGER HORIZONTAL COMPONENT
D. M. BOORE, W. B. JOYNER, AND T. E. FUMAL
(SEE U.S. GEOLOGICAL SURVEY OPEN-FILE REPORT 93-509)

B1SS	BIRV	B1ALL	B2	B3	H	B4	B5	B6	B7	B8	SIG1	SIGE	SIGC
-0.068	0.017	-0.038	0.216	0.000	5.48	0.00000	-0.777	0.158	0.254	0.000	0.194	0.051	0.000

INTRODUCTION

More than a decade ago we presented equations for predicting peak horizontal acceleration and response spectra in terms of moment magnitude, distance, and site conditions for shallow earthquakes in western North America (Joyner and Boore, 1981, 1982). We are currently developing a new set of equations taking account of the data recorded since 1980. In addition to incorporating the new data, we plan to reprocess all the data for greater uniformity and for the purpose of extending the period range to as long a period as possible. Because of the time that will be required to complete the long-term project, we decided to present an interim report (Boore *et al.*, 1993, hereafter referred to as "BJF93") updating our earlier equations to incorporate data from three recent California earthquakes (Loma Prieta, 1989, Petrolia, 1992, and Landers, 1992) that provided data in the large-magnitude, close-distance range where the earlier data set was severely deficient. In addition to including the new data, we changed the site classification system to a three-category classification based on average shear-wave velocity to a depth of 30 m. Other changes are described in BJF93. In order to make the new equations available as soon as possible, we published the interim report before we had completed several auxiliary studies of the data set. Those additional studies are the subject of this report, which we designate as part two of the interim report.

This report contains ten items, summarized below. In general, new topics not contained in BJF93 are discussed first.

1. As an alternative to the three-category site classification, we present a way of calculating the site effect as a continuous function of the average shear-wave velocity to a depth of 30 m.

2. We study residuals within 10 km and perform a Monte Carlo simulation study to see if the scaling with magnitude at close distances is different from that at larger distances.

3. We examine residuals for the BJF93 equations to see if the variance depends on magnitude or if it depends on ground-motion amplitude.

4. We examine differences in ground motion between strike-slip and reverse-slip earthquakes.

5. We perform a Monte Carlo simulation study to assess the sensitivity of the predicted values to stochastic uncertainties in the regression coefficients.

6. We compare response spectra predicted from equations developed by one-stage and two-stage maximum-likelihood methods.

7. We present plots showing how residuals for peak horizontal acceleration depend on magnitude, distance, and site conditions (similar plots were given in BJF93 for response spectra but not for peak acceleration).

8. We include equations for predicting smoothed response spectra in terms of cubic polynomials in period, from which predictions can be obtained for periods not included in BJF93.

9. We discuss limitations of the present equations and prospects for improvement in future work.

10. We include errata for BJF93.

The one-stage and two-stage calculations in this report and in BJF93 were done by the methods described by Joyner and Boore (1993) as corrected (Joyner and Boore, 1994), except that, in the first stage of the two-stage regression, the sum of square errors was minimized with respect to the parameter h in equation (2) of BJF93 by a simple numerical search (using the routine GOLDEN [Press *et al.*, 1992]) rather than by linearization as described in Joyner and Boore (1993).

THE SITE EFFECT IN TERMS OF SHEAR-WAVE VELOCITY

In the equations of BJF93 the site-effect term takes on different values depending on whether the average shear-wave velocity to a depth of 30 m is greater than 750 m/s (Class A), between 360 and 750 m/s (Class B), or between 180 and 360 m/s (Class C). The class definitions are taken from site-effects provisions proposed for the 1994 National Earthquake Hazards Reduction Program (NEHRP) model building-code provisions. (The NEHRP proposal also has a Class D with average velocity less than 180 m/s, but Class D was poorly represented in the BJF93 data set and was excluded from the analysis.) We are confident that the use of a classification system based entirely on shear-wave velocity represents an improvement over systems based on subjective descriptions of site geology. Even though the classification system is an improvement, it would be better still to compute the site effect as a continuous function of shear-wave velocity, if available. We have done that, generally following the ideas of Joyner and Fumal (1984).

For more than half the records used in developing the BJF93 equations the time-weighted average shear-wave velocities to 30 m (V_S) have been obtained from downhole surveys at the sites (a histogram of these velocities is shown in Figure 1, and the recordings used in the analysis are listed in Table 1). The average is computed by dividing 30 m by the S-wave travel time to 30 m (in contrast to a depth-weighted average found by dividing the sum of the product of the layer thickness and velocity by 30 m). For those records, we take the residuals (R) with respect to the BJF93 equations for site Class A and fit the following functional form to the residuals by two-stage regression:

$$\log R = b_V(\log V_S - \log V_A) + \epsilon_r + \epsilon_e. \tag{1}$$

In this equation $\log R$ is the residual (log observed minus log predicted ground motion), ϵ_r is an independent random variable that takes on a specific value for each record, and ϵ_e is an independent random variable that takes on a specific value for each earthquake. The coefficients to be determined are b_V and $\log V_A$. In the first stage of the two-stage regression the coefficient b_V is determined along with a set of amplitude factors, one for each earthquake. In the second stage a weighted average of the amplitude factors gives the product$(-b_V \log V_A)$ from which V_A is obtained. The weight w_i for each earthquake is given by

$$w_i = (\sigma_1^2/N_{r_i} + \sigma_e^2)^{-1}, \tag{2}$$

where σ_1^2 is the variance of the first stage, N_{r_i} is number of recordings for earthquake i, and σ_e^2 is the intrinsic variance of the amplitude factors. The value of σ_e^2 was determined by requiring that the weighted sum of square deviations of the amplitude factors from the mean be equal (or as close as possible to) the number of degrees of freedom, $N_e - 1$, where N_e is the number of earthquakes. To show graphically the amplification as a function of velocity, we removed the earthquake-to-earthquake variation by subtracting from the residuals a constant given by evaluating, at a velocity equal to V_A, the straight-line fit determined for each earthquake in the first stage of the regression. Figure 2 shows the results for 5 percent damping and a set of eight oscillator periods uniformly distributed logarithmically between 0.1 and 2 seconds (we use this set of periods for many of the graphical results shown in this report). The plots show strong correlation of long-period ground motion with shear-wave velocity. The values of b_V and $\log V_A$ are smoothed by least-squares fitting of a cubic polynomial as was done for the coefficients of the BJF93 equations. The results are given in Table 2 for response spectra and Table 3 for peak acceleration. The term

$$b_V(\log V_S - \log V_A) \quad (3)$$

replaces the term

$$b_6 G_B + b_7 G_C$$

in equation (1) of BJF93. The effect on the variance is negligible, and the standard deviation values from Tables 7, 8, and 9 of BJF93 should be used for these computations as well. (The equations in BJF93 give pseudo-velocity response spectra (*psv*); acceleration spectra (S_A), defined as $(2\pi/T)psv$, can be obtained by adding the column labeled "BSA" in Table 2 to equation (1) in BJF93, where the units of S_A are the acceleration of gravity (g).)

The dependence of the amplification on shear velocity is given by the coefficient b_V in equation (3). As shown in Figure 3, the velocity dependence is remarkably similar to that determined by Midorikawa (written comm., 1993) in Japan and to the coefficients proposed by Borcherdt (1994) for use in determining short- and mid-period amplification factors in building codes.

MAGNITUDE SCALING AT SHORT DISTANCES

Equations given by many authors for predicting ground-motion values have smaller magnitude scaling at short distances than at long distances (*e.g.* Campbell and Bozorgnia, 1994). Our equations have the same magnitude scaling at all distances. Until recently there were no data available to constrain the equations for large earthquakes at close distances, and under these circumstances the differences in magnitude scaling could lead to substantial differences in the predicted ground motions. The 1989 Loma Prieta, 1992 Petrolia, and 1993 Landers earthquakes have provided data in the critical large-magnitude, close-distance range, however, limiting the variations in predicted motions permitted by the data. To see if our data set would support a smaller magnitude scaling at short distance, we took residuals at stations within 10 km with respect to the equation determined for the whole data set. We then used the two-stage regression method to find the linear function of magnitude that best fit the residuals. The results are shown in Figure 4 for peak horizontal acceleration and response spectra at 5 percent damping and 8 periods from 0.1 to 2.0 sec. The slopes of the best-fitting straight lines are positive in some cases and negative in others. The absolute value of the slope is less than the standard error of the slope for peak acceleration and for response spectra at all but one of the 8 periods (0.85

sec). We conclude there is no support in the data for smaller magnitude scaling at short distance.

We also used Monte Carlo simulation (Press *et al.*, 1992) to examine the question of magnitude scaling at close distance. A different magnitude scaling at close distance can be obtained by setting the parameter h in equation (2) of BJF93 equal to

$$h_1 \exp(h_2[\mathrm{M} - 6]). \tag{4}$$

We take as our null hypothesis that $h_2 = 0$ and see if that hypothesis is compatible with the data. To do so we start with an input set of parameter values determined by fitting the real data set with h_2 constrained to be zero. We take the magnitude, distance, and site-condition values from the data set and use the input parameter set in equation (1) of BJF93 with the aid of a pseudorandom-number generator to simulate a set of ground-motion values, which we analyze by the two-stage method with h given by equation (4). We do 100 simulations for peak horizontal acceleration and 100 simulations for response spectra at 5 percent damping and each of 8 periods equally spaced logarithmically between 0.1 and 2.0 sec. We then analyze the real data using the two-stage method with h given by equation (4). (In the first stage the sum of square errors is minimized with respect to h_1 and h_2 by the downhill simplex method [Press *et al.*, 1992].) The h_2 values determined from the real data are compared in Figure 5 with the distribution of values simulated under the null hypothesis. For peak acceleration the value determined from the data is at the 31st percentile level of the distribution of simulated values. For the response spectra, the smallest value is at the 6th percentile level, two values are smaller than the 10th percentile level, and the remaining six are less than the 90th percentile level. We see no basis for rejecting the null hypothesis $h_2 = 0$.

THE EFFECT OF MAGNITUDE AND AMPLITUDE ON VARIANCE

Dependence on Magnitude. A number of authors have suggested that the variance of peak horizontal acceleration depends on magnitude (for example, Idriss, 1985, and Youngs *et al.*, 1994, who show that the dependence is statistically significant). We examine the suggestion for our data, using prediction equations derived by the one-stage maximum-likelihood method to make the results comparable to those of Youngs *et al.* (1994). We divide the data into three magnitude classes, 5.00–5.99, 6.00–6.99, and 7.00–7.99, and take the residuals in each class with respect to the equation determined for the whole data set. For each class we determine the variance σ_c^2 of the horizontal components (BJF93, equation [3]). Then for each class we average the residuals of the two horizontal components and use the one-stage maximum-likelihood method to determine σ_e^2, the earthquake-to earthquake component of the variance, and σ_1^2, which represents the remaining components of variability. The total variance $\sigma_{\log Y}^2$ is equal to $\sigma_1^2 + \sigma_e^2 + \sigma_c^2$. To estimate the standard error of the total variance we use the large-sample expressions given by Searle (1971, p.474) for the variance of σ_1^2 and σ_e^2 and the covariance of σ_1^2 and σ_e^2, and we assume that σ_c^2 is independent of σ_1^2 and σ_e^2, an assumption that may not be strictly correct. The results for peak horizontal acceleration and response spectral values at eight periods are given in Figure 6, which shows the estimate of $\sigma_{\log Y}$ for each magnitude class with error bars corresponding to plus and minus one standard error of $\sigma_{\log Y}^2$. For peak acceleration we, like Youngs *et al.* (1994), find that $\sigma_{\log Y}$ decreases with increasing magnitude and we, like they, find that most of the effect appears below magnitude 6.0. For response spectral values we see no significant dependence of variance on magnitude. The difference between the results for peak acceleration and response spectral values is probably due, at least in part, to the relatively few records in the response spectral data set from earthquakes with magnitude less than 6.0 (1 and 5 records from earthquakes of magnitude 5.3 and 5.8, respectively; see Figure 1 in BJF93).

Dependence on Amplitude. Some authors have suggested that the variance of peak horizontal acceleration depends on the value of peak acceleration (Donovan and Bornstein, 1978; Campbell and Bozorgnia, 1994). We examine our peak acceleration data for such dependence using equation (1) in BJF93. We divide the data into three classes, using a three-to-one ratio between the values defining the middle class: 1) those records for which the predicted peak acceleration is less than 0.1 g, 2) those for which the predicted value falls between 0.1 and 0.3 g, and 3) those for which the predicted value is greater than or equal to 0.3 g. As above we determine, for each class, the variance σ_c^2 of the horizontal components (BJF93, equation [3]). Then, for each class, we average the residuals of the two horizontal components and use the one-stage maximum-likelihood method to determine σ_e^2, the earthquake-to earthquake component of the variance, and σ_1^2 which represents the remaining components of variability. We also study the response-spectral data for evidence of an amplitude-dependent variance. As before, we maintain a three-to-one ratio between the boundary values used to define the middle amplitude class and adjust the values to maintain a sufficient number of data points in each category. The boundary values, which depend on oscillator period, are given in Table 4. The values of $\sigma_{\log Y}^2$ for each class are determined as described above. The results for peak horizontal acceleration and response spectral values at eight periods are given in Figure 7, which shows the estimate of $\sigma_{\log Y}$ for each amplitude class with error bars corresponding to plus and minus one standard error of $\sigma^2_{\log Y}$. For peak acceleration we, like Campbell and Bozorgnia (1994), find that $\sigma_{\log Y}$ decreases with increasing peak acceleration. Figure 7 shows that most of the effect for peak acceleration with our data set appears for Amplitude Class 1 (below 0.1 g). For response spectra our data set shows no clear trend. The difference between peak acceleration and response spectra reflects in part the relatively fewer low-amplitude data points in the response spectral data set.

THE EFFECT OF FOCAL MECHANISM ON RESPONSE SPECTRAL VALUES

Many authors (most recently Campbell and Bozorgnia, 1994) have proposed that ground-motion values depend on the focal mechanism of the earthquake. We examine that proposition for response spectra. Table 5 gives the rake angles for the earthquakes in the response spectral data set, using the convention of Aki and Richards (1980) that reverse slip earthquakes have positive rake angles, and the absolute value of the rake for left-lateral slip is less than 90 degrees. The rake angle for the Daly City earthquake is indeterminate (given by 999 in Table 5), because the fault plane is indistinguishable from horizontal. We define strike-slip earthquakes as those with a rake angle within 30 degrees of horizontal. The remaining earthquakes are reverse-slip, because there are no normal-slip events in the data set. We do a two-stage regression analysis using equation [1] in BJF93, except in the second stage we replace the constant term b_1 by $b_{SS}G_{SS} + b_{RS}G_{RS}$, where $G_{SS} = 1$ for a strike-slip earthquake and zero otherwise, $G_{RS} = 1$ for a reverse-slip earthquake and zero otherwise, and b_{SS} and b_{RS} are coefficients to be determined. The magnitude-dependence given by coefficients b_2 and b_3 values need not be the same as before. In fact, for all periods the quadratic magnitude dependence (b_3) is small compared to the uncertainty in the coefficient. For this reason, we reran the problem constraining b_3 to be zero. The ratio of the response spectral values between reverse- and strike-slip earthquakes (Y_{RS}/Y_{SS}) is given by 10 raised to the power $b_{RS} - b_{SS}$. This ratio is plotted against period in Figure 8. The error bars represent plus and minus one standard deviation. Figure 8 shows that the response spectral values are larger for reverse-slip earthquakes than for strike-slip earthquakes, but the differences are relatively small and of marginal significance statistically. We await our future analysis using the more complete data set before deciding whether or not focal mechanism should be used as a predictor variable.

SENSITIVITY OF PREDICTION ERROR TO PARAMETER UNCERTAINTY

We used Monte Carlo simulation (Press *et al.*, 1992) to evaluate the contribution to prediction error from stochastic uncertainty in the parameters of the prediction equations. We start with an input set of parameter values determined by fitting the real data set. We take the magnitude, distance, and site-condition values from the data set and use the input parameter set in equation (1) of BJF93 with the aid of a pseudorandom-number generator to simulate a set of ground-motion values, which we analyze by the two-stage method to obtain a set of simulated parameters. We then use the set of simulated parameters to predict ground-motion values at Class C sites for $\mathbf{M} = 6.5$ and 7.5 at $d = 0$ and 20 km. We used 100 simulations for peak horizontal acceleration and 100 simulations for response spectra at 5 percent damping and each of 8 periods from 0.1 to 2.0 sec. The mean predicted values of the ground motions from the simulations are within about 3% of the ground-motion values predicted from the input parameters. This close agreement indicates that there is no bias introduced by the particular distribution of the data set over magnitude, distance, and site condition and no bias introduced by the analysis method. The contribution to prediction error from stochastic uncertainties in the parameters is less than 35 percent for $d = 0$ km and substantially less at $d = 20$ km. These contributions are small compared to the standard error of an individual prediction.

RESIDUALS OF PEAK HORIZONTAL ACCELERATION

Figure 9 gives the average residual for the two horizontal components of peak acceleration plotted against distance for different site and magnitude classes for the prediction equations of BJF93. Similar plots were presented in BJF93 for response spectra at 0.3 s and 1.0 s and 5-percent damping.

PREDICTION EQUATIONS AS CONTINUOUS FUNCTIONS OF PERIOD

Even though we evaluated the regression coefficients at a relatively dense set of oscillator periods, for some purposes it may be desired to predict response spectra at other periods. A convenient way to do this is to take advantage of our smoothing of the coefficients over period. As discussed in BJF93, we settled on fitting the regression coefficients by cubic polynomials in $\log T$ as follows:

$$B = C_0 + C_1 \log(T/0.1) + C_2(\log(T/0.1))^2 + C_3(\log(T/0.1))^3, \tag{5}$$

where B is a regression coefficient. We give the polynomial coefficients for the prediction of response spectra in terms of site classes in Tables 6 and 7 and in terms of average-shear wave velocity in Tables 8 and 9. These coefficients should *not* be used to predict response spectra outside of the period range from 0.1 to 2.0 sec (where the coefficients were determined). Extension of the cubic polynomial outside that range is likely to lead to ridiculous results.

COMPARISON OF ONE-STAGE AND TWO-STAGE MAXIMUM-LIKELIHOOD METHODS

The equations for response spectra given in BJF93 were obtained with the two-stage maximum-likelihood method. One-stage maximum-likelihood methods have been proposed (for example, Brillinger and Preisler, 1984, 1985), and we here compare spectra obtained using one-stage and two-stage methods (for the one-stage method we used the procedure described in Joyner and Boore, 1993). The results were very similar as illustrated by Figure 10, which compares unsmoothed, five-percent-damped spectra for the random horizontal component computed using the one-stage method (heavy lines) with spectra computed using the two-stage method (light lines) for a C site in a magnitude 7.5 earthquake at distances of 0, 10, 20, 40, and 80 km.

LIMITATIONS OF THE PRESENT WORK AND PROSPECTS FOR IMPROVEMENT

Few response spectral data below magnitude 6.0. Earthquakes with magnitudes less than 6.0 are poorly represented in the response-spectral data set, which includes only one record from a magnitude 5.3 earthquake and six records from a magnitude 5.8 earthquake. Prediction of ground motion for the smaller earthquakes is less important, of course, but it would be desirable to increase the number of data for small earthquakes. This will be accomplished when we add all the recently recorded earthquakes to the data set.

Few Class A data. Ground-motion predictions for Class A are not as well determined as for the other classes because there are very few Class A sites. In the response-spectral data set there are 11 Class A sites, 49 Class B sites, and 46 Class C sites. (The total number of sites is less than the total number of records because some sites recorded more than one earthquake.) The residual plots for class A data (Figure 9) suggest that the predictions may be somewhat low within about 12 km for peak acceleration. When we add all the recently recorded earthquakes to the data set, we will increase the number of Class A data, but there will always be fewer data in Class A than in the other classes.

Poor distribution of Class D sites. We did not include records from Class D sites in the data analysis, because those records were available from only one earthquake (Loma Prieta) and only from a limited area and we could not presume that they constituted a representative sample. This situation will not improve until more recordings are made at Class D sites. The Loma Prieta Class D recordings were used by Joyner *et al.* (1994) to estimate site effects on response spectral values by comparison with recordings at other nearby sites.

Effect of site conditions on short-period motion. The equations developed from our current data set show differences between site classes for peak acceleration and for response spectra at all periods, while the earlier equations showed little or no difference for peak acceleration or for response spectra at periods 0.3 sec and smaller. The change is the result of adding new data, and it is an improvement in the sense that the new data set includes a broader range of site conditions. The particular way in which site conditions affect short-period motions, however, may depend on variables not included in the prediction equations. For example, two sites may have the same average shear velocity over the upper 30 m, but they may be underlain by different thicknesses of attenuating material. For a large enough thickness, the effect of anelastic attenuation on short-period motions may largely offset, or even reverse, the effect of amplification. When we add all the recently-recorded earthquakes to the data set and compile all the available geologic site data, we will try adding a variable representing the thickness of attenuating material to the equations.

Averaging velocity over 30 m. The use of average shear-wave velocity to a depth of 30 m as a variable to characterize site conditions is a choice dictated by the relative unavailability of velocity data for greater depths. The ideal parameter would be average shear-wave velocity to a depth of one-quarter wavelength for the period of interest, as was used by Joyner and Fumal (1984; see also Boore and Joyner, 1991). By the quarter-wavelength rule, 30 m is the appropriate depth for periods less than 0.16 sec for Class A, periods between 0.16 and 0.33 sec for Class B, and periods between 0.33 and 0.67 sec for Class C. The use of shear-wave velocity averaged over 30 m may work reasonably well for other depths and periods, because it will have a high correlation with the average over greater depths. We hope, however, to develop estimates of average shear-wave velocity to greater depths at a sufficient number of sites so that we can ultimately provide ground-motion prediction equations in terms of average shear-wave velocity to a depth of one-quarter wavelength.

Distance limitations. There are very few recordings in the data set for distances greater than 100 km, and we recommend that the equations not be used for greater distances. Such a limitation is inherent in the strong-motion data set as long as it is dominated by conventional triggered instruments. In our future work we hope to extend the range of our predictions to larger distances by using weak-motion data recorded on seismographic networks to obtain the attenuation of ground motion with distance in combination with stochastic methods (e.g., Hanks and McGuire, 1981; Boore, 1983) to define the magnitude scaling. The magnitude scaling at distances beyond about 100 km may be somewhat greater than at closer distances for two reasons: the periods controlling the oscillator response may increase because of anelastic attenuation, and the energy radiated by the earthquake may be spread over a longer duration. An example of the distance-dependence of the magnitude scaling can be seen in Figure 9 of Atkinson and Boore (1990).

Basin-generated surface waves. Surface waves have been recorded by strong-motion instruments at sites in deep sedimentary basins (Hanks, 1975). These waves arrive later than the S body waves and have periods in the general range of 3–10 sec. In some, perhaps most, cases these waves are generated at the margins of the sedimentary basins by conversion from body waves in the high-velocity material bounding the basin (Vidale and Helmberger, 1988; Frankel *et al.*, 1991). At some sites the largest amplitudes at long periods may be due to surface waves. Surface waves are probably not significant for the periods covered by the equations in BJF93 and the present report (two seconds and less), but they represent an important issue in ground-motion prediction.

Effect of distance cutoffs that are independent of geology and azimuth. The limits on the distance range within which our equations may be used for predicting ground motion are made more severe by our attempt to avoid bias due to instruments that do not trigger. To avoid that bias, we exclude from the data set for each earthquake all records obtained at distances equal to or greater than the closest operational instrument that did not trigger or that triggered on the S wave. We use different cutoff distances for stations employing a trigger sensitive to horizontal motion and those with a trigger sensitive to vertical motion, but for simplicity we use cutoff distances independent of geologic site conditions and independent of azimuth (see BJF93). Because amplitude depends on site conditions and on azimuth through the effects of radiation pattern and directivity, the use of cutoff distances independent of geology and azimuth may result in the unnecessary exclusion of records. We choose simplicity and objectivity, however, over increasing the number of records in the data set, and we believe avoiding bias is far more important than increasing the number of data. Alternative methods of avoiding bias are available that do not require the exclusion of records (Toro, 1981; McLaughlin, 1991). Although these methods add significantly to the complexity of the analysis we may consider these methods in our future work. They will become largely unnecessary, however, if we have functions giving ground-motion distance dependence developed by stochastic methods with the help of data other than strong-motion data, as described above.

ERRATA FOR BJF93

Here is a list of typographical errors and omissions in BJF93 known to us at this time:

p. 4, l. 2: Delete extra ".".

p. 5, l. 10 from bottom: Records for which only a single horizontal component was available were not deleted if the other component was not operational.

p. 7, l. 4: Replace extra "i" with "n" in "wiinowed".

p. 11, last line: Replace "Agency" with "Commission".

Tables 4 and 5: The Anderson Dam recording of the Loma Prieta earthquake was obtained at the downstream site.

Table 6: The latitude of Hole 131 (Gilroy #7) should be 37.033.

Table 6: The information used to assign average shear-wave velocity to those boreholes with a reference to "EPRI/CUREE" was preliminary, and has been superseded by the report by Thiel and Schneider (1993). The average velocity at all sites has changed, and in four cases the new shear-wave velocities have produced a change in site class. Table 10 contains those sites that change class, and Table 11 gives updated borehole information (including some sites not used in the regression analysis). We determined that the changes had no significant effect on the equations in BJF93, and for that reason we chose not to include corrected equations in this paper.

ACKNOWLEDGMENTS

We wish to thank Norm Abrahamson and Ken Campbell for their comments, Charles Mueller for his review of the manuscript, and S. Midorikawa for providing data plotted in

Figure 3. This work was partially supported by the U.S. Nuclear Regulatory Commission.

REFERENCES

Aki, K. and P. G. Richards (1980). *Quantitative Seismology Theory and Methods* **1**, 557 p., W. H. Freeman and Company.

Algermissen S. T., J. W. Dewey, C. J. Langer, and W. H. Dillinger (1974). The Managua, Nicaragua, earthquake of December 23, 1972: Location, focal mechanism, and intensity distribution, *Bull. Seism. Soc. Am.* **64**, 993–1004

Allen, C. R. and J. M. Nordquist (1972). Foreshock, main shock, and larger aftershocks of the Borrego Mountain earthquake, *U. S. Geol. Surv. Prof. Paper 787*, 16–23.

Archuleta, R. J. (1984). A faulting model for the 1979 Imperial Valley earthquake, *J. Geophys. Res.* **89**, 4559–4585.

Atkinson, G. M. and D. M. Boore (1990). Recent trends in ground motion and spectral response relations for North America, *Earthquake Spectra* **6**, 15–35.

Boore, D. M. (1983). Stochastic simulation of high-frequency ground motions based on seismological models of the radiated spectra, *Bull. Seism. Soc. Am.* **73**, 1865–1894.

Boore, D. M. and D. J. Stierman (1976). Source parameters of the Pt. Mugu, California, earthquake of February 21, 1973, *Bull. Seism. Soc. Am.* **66**, 385–404.

Boore, D. M. and W. B. Joyner (1991). Estimation of ground motion at deep-soil sites in eastern North America, *Bull. Seism. Soc. Am.* **81**, 2167–2185.

Boore, D. M., W. B. Joyner, and T. E. Fumal (1993). Estimation of response spectra and peak accelerations from western North American earthquakes: An interim report, *U. S. Geol. Surv. Open-File Rept. 93-509*, 72 pp.

Borcherdt, R. D. (1994). Simplified site classes and empirical amplification factors for site-dependent code provisions, *Proceedings NCEER/SEAOC/BSSC Workshop on Site Response During Earthquakes and Seismic Code Provisions*, University of Southern California, November 18–20, 1992, (in press).

Brillinger, D. R. and H. K. Preisler (1984). An exploratory analysis of the Joyner-Boore attenuation data, *Bull. Seism. Soc. Am.* **74**, 1441–1450.

Brillinger, D. R. and H. K. Preisler (1985). Further analysis of the Joyner-Boore attenuation data, *Bull. Seism. Soc. Am.* **75**, 611–614.

Campbell, K. W. and Y. Bozorgnia (1994). Near-source attenuation of peak horizontal acceleration from worldwide accelerograms recorded from 1957 to 1993, Proc. Fifth U. S. National Conference on Earthquake Engineering, Chicago, Illinois, July 10-14, 1994 (in press).

Cockerham, R. S., F. W. Lester, and W. L. Ellsworth (1980). A preliminary report on the Livermore Valley earthquake sequence January 24–February 26, 1980, *U. S. Geol. Surv. Open-File Rept. 80-714*.

Corbett, E. J. and C. E. Johnson (1982). The Santa Barbara, California, earthquake of 13 August 13 1978, *Bull. Seism. Soc. Am.* **72**, 2201-2226.

Donovan, N. C. and A. E. Bornstein (1978). Uncertainties in seismic risk procedures, *Proc. Am. Soc. Civil Eng., J. Geotech. Eng. Div.* **104**, 869–887.

Dunbar, W. S., D. M. Boore, and W. Thatcher (1980), Pre-, co-, and postseismic strain changes associated with the 1952 $M_L = 7.2$ Kern County, California, earthquake, *Bull. Seism. Soc. Am.* **70**, 1893–1905.

Frankel, A., S. Hough, P. Friberg, and R. Busby (1991). Observations of Loma Prieta aftershocks from a dense array in Sunnyvale, California *Bull. Seism. Soc. Am.* **81**, 1900–1922.

Given, D. D. (1983). Seismicity and structure of the trifurcation in the San Jacinto fault zone, southern California, *M.S. thesis, Cal. State University, Los Angeles*, 73 p.

Hanks, T. C. (1975). Strong ground motion of the San Fernando, California, earthquake: ground displacements, *Bull. Seism. Soc. Am.* **65**, 193–225.

Hanks, T. C. and R. K. McGuire (1981). The character of high frequency strong ground motion, *Bull. Seism. Soc. Am.* **71**, 2071–2095.

Hasegawa, H. S., J. C. Lahr, and C. D. Stephens (1980). Fault parameters of the St. Elias, Alaska, earthquake of February 28, 1979, *Bull. Seism. Soc. Am.* **70**, 1651–1660.

Heaton, T. H. (1982). The 1971 San Fernando earthquake: A double event?, *Bull. Seism. Soc. Am.* **72**, 2037–2062.

Idriss, I. M. (1985). Evaluating seismic risk in engineering practice, *Proc. Eleventh Internat. Conf. on Soil Mech. and Foundation Eng.*, August 12–16, 1985, San Francisco, California, **1**, 255–320, A. A. Balkema, Rotterdam.

Joyner, W.B. and D.M. Boore (1981). Peak acceleration and velocity from strong-motion records including records from the 1979 Imperial Valley, California, earthquake, *Bull. Seism. Soc. Am.* **71**, 2011–2038.

Joyner, W.B. and D.M. Boore (1982). Prediction of earthquake response spectra, *U. S. Geol. Surv. Open-File Rept. 82-977*, 16 p.

Joyner, W.B. and D.M. Boore (1993). Methods for regression analysis of strong-motion data, *Bull. Seism. Soc. Am.* **83**, 469–487.

Joyner, W. B. and D. M. Boore (1994). Errata, *Bull. Seism. Soc. Am.* **84**, (in press).

Joyner, W. B. and T. E. Fumal (1984). Use of measured shear-wave velocity for predicting geologic site effects on strong ground motion, *Proc. Eighth World Conf. on Earthquake Eng. (San Francisco)* **2**, 777–783.

Joyner, W. B., T. E. Fumal, and G. Glassmoyer (1994). Empirical spectral response ratios for strong-motion data from the 1989 Loma Prieta, California, earthquake, *Proceedings NCEER/SEAOC/BSSC Workshop on Site Response During Earthquakes and Seismic Code Provisions*, Los Angeles, November 18–20, 1992 (in press).

Kanamori, H., H. K. Thio, D. Dreger, E. Hauksson, and T. Heaton (1992). Initial investigation of the Landers, California, earthquake of 28 June 1992 using TERRAscope, *Geophys. Res. Lett. 19*, 2267–2270.

Langston, C. A. (1978). The February 9, 1971 San Fernando earthquake: A study of source finiteness in teleseismic body waves, *Bull. Seism. Soc. Am.* **68**, 1–29.

Lee, W. H. K. (1974). A preliminary study of the Hollister earthquake of November 28, 1974 and its major aftershocks, (unpublished manuscript dated December 6, 1974).

Liu, H-L and D. V. Helmberger (1983). The near-source ground motion of the 6 August 1979 Coyote Lake, California, earthquake, *Bull. Seism. Soc. Am.* **73**, 201–218.

McEvilly, T. V. (1966). Preliminary seismic data June-July, 1966, Monterey and San Luis Obispo Counties, California, preliminary report, *Bull. Seism. Soc. Am.* **56**, 967–971.

McLaughlin, K. L. (1991). Maximum likelihood estimation of strong-motion attenuation relationships, *Spectra* **7**, 267–279.

Oppenheimer, D., G. Beroza, G. Carver, L. Dengler, J. Eaton, L. Gee, F. Gonzalez, A. Jayko, W. H. Li, M. Lisowski, M. Magee, G. Marshall, M. Murray, R. McPherson, B. Romanowicz, K. Satake, R. Simpson, P. Somerville, R. Stein, and D. Valentine (1993). The Cape Mendocino, California, earthquakes of April 1992: Subduction at the triple junction, *Science* **261**, 433–438.

Press, W.H., B.P. Flannery, S.A. Teukolsky, and W.T. Vetterling (1986). *Numerical Recipes, the Art of Scientific Computing*, Cambridge University Press, Cambridge, U.K.

Richter, C. F. (1958). *Elementary Seismology*, W. H. Freeman and Company, San Francisco, 768 pp.

Schell, M. M. and L. J. Ruff (1986). Southeastern Alaska tectonics: Source process of the large 1972 Sitka earthquake (abs), *Eos (Trans. Amer. Geophys. Un.)* **67**, 304.

Searle, S. R. (1971). *Linear Models*, Wiley, New York, 532 pp.

Stein, R. S. and W. Thatcher (1981). Seismic and aseismic deformation associated with the 1952 Kern County, California, earthquake and relationship to the quaternary history of the White Wolf fault, *J. Geophys. Res.* **86**, 4913–4928.

Thiel Jr., C. C. and J. F. Schneider (1993). Investigations of Thirty-Three Loma Prieta Earthquake Strong Motion Recording Sites, final report of project sponsored by the Building Contractors Society of Japan and the Electric Power Research Institute, California Universities for Research in Earthquake Engineering (CUREe), Dept. of

Civil Engineering, Stanford Univ., Stanford, Calif.

Toro, G. R. (1981). Biases in seismic ground motion prediction, Massachusetts Institute of Technology, Department of Civil Eng. Res. Rept. R81-22, Cambridge, Massachusetts, 133 p.

Uhrhammer, R. A. (1981). The Pacifica earthquake of 28 April 1979, *Bull. Seism. Soc. Am.* **71**, 1161–1172.

Vidale, J. E. and D. V. Helmberger (1988). Elastic finite-difference modeling of the 1971 San Fernando, California, earthquake, *Bull. Seism. Soc. Am.* **78**, 122–141.

Wallace, T. C., A. Velasco, J. Zhang, and T. Lay (1991). A broadband seismological investigation of the 1989 Loma Prieta, California, earthquake: Evidence for deep slow slip?, *Bull. Seism. Soc. Am.* **81**, 1622–1646.

Whitcomb, J. H. (1971). Fault-plane solutions of the February 9, 1971, San Fernando earthquake and some aftershocks, *U. S. Geol. Surv. Prof. Paper 733*, 30–32.

Youngs, R. R., N. Abrahamson, F. Makdisi, and K. Sadigh (1994). Magnitude-dependent variance of peak ground acceleration, *Bull. Seism. Soc. Am.* **84**, (in press).

Table 1. Records used in the development of the equations for response spectra as a continuous function of average shear velocity.

DATE	EARTHQUAKE	M	DIST	STATION	LAT.	LONG.	G	AVGVEL	HOLE	SOURCE
19-May-40	Imperial Vall	7.00	12.0	El Centro Array Sta 9	32.794	115.549	C	213	107	n
21-Jul-52	Kern County	7.40	42.0	Taft	35.150	119.460	B	429	201	n
21-Jul-52	Kern County	7.40	85.0	Santa Barbara	34.420	119.700	B	508	96	n
21-Jul-52	Kern County	7.40	109.0	Pasadena - Athenaeum	34.140	118.120	B	417	92	n
21-Jul-52	Kern County	7.40	107.0	Hollywood Storage Bldg PE Lo	34.090	118.340	C	318	63	n
22-Mar-57	Daly City	5.30	8.0	San Fran.: Golden Gate Park	37.770	122.480	A	783	173	n
28-Jun-66	Parkfield	6.10	16.1	Cholame-Shandon: Temblor	35.710	120.170	B	509	200	n
28-Jun-66	Parkfield	6.10	6.6	Parkfield: Cholame 2	35.733	120.288	C	194	228	n
28-Jun-66	Parkfield	6.10	9.3	Parkfield: Cholame 5W	35.697	120.328	C	278	197	n
28-Jun-66	Parkfield	6.10	13.0	Parkfield: Cholame 8W	35.671	120.359	C	260	198	n
9-Apr-68	Borrego Mount	6.60	45.0	El Centro Array Sta 9	32.794	115.549	C	213	107	n
9-Feb-71	San Fernando	6.60	17.0	Lake Hughes Sta 12	34.570	118.560	B	600	86	n
9-Feb-71	San Fernando	6.60	25.7	Pasadena - Athenaeum	34.140	118.120	B	417	92	n
9-Feb-71	San Fernando	6.60	60.7	Wrightwood	34.360	117.630	B	482	88	n
9-Feb-71	San Fernando	6.60	19.6	Lake Hughes Sta 4	34.650	118.478	C	351	71	n
6-Aug-79	Coyote Lake	5.80	9.1	Gilroy Array 1	36.973	121.572	A	1415	192	n
6-Aug-79	Coyote Lake	5.80	1.2	Gilroy Array 6	37.026	121.484	B	714	196	n
6-Aug-79	Coyote Lake	5.80	3.7	Gilroy Array 4	37.005	121.522	C	223	195	n
6-Aug-79	Coyote Lake	5.80	5.3	Gilroy Array 3	36.987	121.536	C	306	194	n
6-Aug-79	Coyote Lake	5.80	7.4	Gilroy Array 2	36.982	121.556	C	309	193	n
15-Oct-79	Imperial Vall	6.50	14.0	Parachute Test Site	32.929	115.699	B	370	116	n
15-Oct-79	Imperial Vall	6.50	.6	El Centro Array Sta 7	32.829	115.504	C	211	105	n
15-Oct-79	Imperial Vall	6.50	1.3	El Centro Array Sta 6	32.839	115.487	C	201	104	n
15-Oct-79	Imperial Vall	6.50	2.6	Bonds Corner	32.693	115.338	C	224	97	n
15-Oct-79	Imperial Vall	6.50	3.8	El Centro Array Sta 8	32.810	115.530	C	205	106	n
15-Oct-79	Imperial Vall	6.50	4.0	El Centro Array Sta 5	32.855	115.466	C	207	103	n
15-Oct-79	Imperial Vall	6.50	5.1	El Centro: Differential Arra	32.796	115.535	C	200	112	n
15-Oct-79	Imperial Vall	6.50	6.8	El Centro Array Sta 4	32.864	115.432	C	211	102	n
15-Oct-79	Imperial Vall	6.50	7.5	Holtville	32.812	115.377	C	201	99	n
15-Oct-79	Imperial Vall	6.50	8.5	El Centro Array Sta 10	32.780	115.567	C	203	108	n
15-Oct-79	Imperial Vall	6.50	8.5	Brawley	32.991	115.512	C	210	114	n
15-Oct-79	Imperial Vall	6.50	12.6	El Centro Array Sta 11	32.752	115.594	C	196	109	n
15-Oct-79	Imperial Vall	6.50	16.0	El Centro Array Sta 2	32.916	115.366	C	190	100	n
15-Oct-79	Imperial Vall	6.50	18.0	El Centro Array Station 12	32.718	115.637	C	210	110	n
15-Oct-79	Imperial Vall	6.50	22.0	El Centro Array Sta 13	32.709	115.683	C	252	111	n
15-Oct-79	Imperial Vall	6.50	23.0	Calipatria	33.130	115.520	C	197	117	n
18-Oct-89	Loma Prieta	6.92	10.5	Gilroy Array 1	36.973	121.572	A	1415	192	c
18-Oct-89	Loma Prieta	6.92	42.7	Monterey City Hall	36.597	121.897	A	763	209	c
18-Oct-89	Loma Prieta	6.92	67.6	S. San Fran.: Sierra Pt.	37.674	122.388	A	1020	220	c

18-Oct-89	Loma Prieta	6.92	0.0	Corralitos	37.046	121.803	B	460	130	c
18-Oct-89	Loma Prieta	6.92	19.9	Gilroy Array 6	37.026	121.484	B	714	196	c
18-Oct-89	Loma Prieta	6.92	20.0	Anderson Dam: Downstream	37.166	121.628	B	506	142	u
18-Oct-89	Loma Prieta	6.92	34.1	SAGO South A	36.753	121.396	B	612	211	c
18-Oct-89	Loma Prieta	6.92	36.1	Calaveras Reservoir South	37.452	121.807	B	482	143	u
18-Oct-89	Loma Prieta	6.92	38.7	Woodside	37.429	122.258	B	455	132	c
18-Oct-89	Loma Prieta	6.92	42.0	Mission San Jose	37.530	121.919	B	368	224	c
18-Oct-89	Loma Prieta	6.92	46.4	APEEL Array Sta 9	37.478	122.321	B	454	1	u
18-Oct-89	Loma Prieta	6.92	46.5	APEEL Array Sta 7	37.484	122.313	B	435	164	c
18-Oct-89	Loma Prieta	6.92	46.6	APEEL Array Sta 10	37.465	122.343	B	401	12	c
18-Oct-89	Loma Prieta	6.92	48.7	Belmont	37.512	122.308	B	628	210	c
18-Oct-89	Loma Prieta	6.92	49.9	Sunol Fire Station	37.597	121.880	B	405	141	u
18-Oct-89	Loma Prieta	6.92	53.7	Bear Valley Sta 5	36.673	121.195	B	391	145	u
18-Oct-89	Loma Prieta	6.92	56.0	APEEL Array Sta 3E	37.657	122.061	B	522	158	c
18-Oct-89	Loma Prieta	6.92	58.7	Hayward City Hall: N. FF	37.679	122.082	B	743	137	u
18-Oct-89	Loma Prieta	6.92	8.6	Capitola	36.974	121.952	C	289	219	c
18-Oct-89	Loma Prieta	6.92	12.1	Gilroy Array 2	36.982	121.556	C	309	193	c
18-Oct-89	Loma Prieta	6.92	14.0	Gilroy Array 3	36.987	121.536	C	306	194	c
18-Oct-89	Loma Prieta	6.92	15.8	Gilroy Array 4	37.005	121.522	C	223	195	c
18-Oct-89	Loma Prieta	6.92	24.3	Gilroy Array 7	37.033	121.434	C	333	131	c
18-Oct-89	Loma Prieta	6.92	25.4	Hollister: Airport	36.888	121.413	C	218	147	u
18-Oct-89	Loma Prieta	6.92	27.0	Agnew	37.397	121.952	C	264	221	c
18-Oct-89	Loma Prieta	6.92	27.5	Sunnyvale	37.402	122.024	C	268	136	u
18-Oct-89	Loma Prieta	6.92	29.3	Halls Valley	37.338	121.714	C	265	230	c
18-Oct-89	Loma Prieta	6.92	34.8	Palo Alto: 2-Story Office Bl	37.453	122.112	C	207	128	c
18-Oct-89	Loma Prieta	6.92	35.0	Stanford: SLAC Test Lab	37.419	122.205	C	344	134	u
18-Oct-89	Loma Prieta	6.92	42.4	Fremont	37.535	121.929	C	283	140	u
18-Oct-89	Loma Prieta	6.92	50.9	Bear Valley Sta 12	36.658	121.249	C	330	144	u
18-Oct-89	Loma Prieta	6.92	56.3	APEEL Array Sta 2E	37.657	122.083	C	276	150	c
18-Oct-89	Loma Prieta	6.92	63.2	San Fran.: Airport	37.622	122.398	C	224	123	c
18-Oct-89	Loma Prieta	6.92	67.3	Bear Valley Sta 10	36.532	121.143	C	311	146	u

AVGVEL is the time-weighted shear velocity averaged over the upper 30 m, in units of meters/second.
SOURCE is expanded in the footnote to Table 5 in BJF93.

Table 2. Smoothed coefficients for response spectra
(psv in cm/s; sa in g; shear velocity in m/s)

		random, 02%		random, 05%		random, 10%		random, 20%		larger, 02%		larger, 05%		larger, 10%		larger, 20%	
T(s)	BSA	BV	VA	BV	VA	BV	VA	BV	VA	BV	VA	BV	VA	BV	VA	BV	VA
.10	-1.193	-.191	970	-.212	1110	-.222	1310	-.251	1510	-.188	950	-.207	1080	-.215	1220	-.232	1540
.11	-1.234	-.189	1160	-.211	1290	-.225	1470	-.255	1620	-.184	1160	-.206	1280	-.218	1430	-.234	1720
.12	-1.272	-.191	1340	-.215	1450	-.230	1600	-.261	1710	-.185	1370	-.209	1470	-.224	1610	-.238	1870
.13	-1.307	-.197	1500	-.221	1600	-.238	1710	-.269	1790	-.190	1560	-.214	1640	-.230	1760	-.243	2000
.14	-1.339	-.205	1640	-.228	1720	-.247	1810	-.277	1850	-.196	1730	-.221	1790	-.238	1900	-.250	2110
.15	-1.369	-.214	1760	-.238	1820	-.257	1880	-.287	1900	-.204	1870	-.229	1910	-.247	2010	-.257	2200
.16	-1.397	-.225	1860	-.248	1910	-.267	1950	-.296	1940	-.214	2000	-.238	2020	-.256	2110	-.265	2280
.17	-1.423	-.236	1950	-.258	1980	-.278	2000	-.306	1970	-.224	2100	-.247	2110	-.265	2190	-.273	2330
.18	-1.448	-.248	2020	-.270	2040	-.289	2040	-.316	1990	-.235	2190	-.257	2180	-.274	2250	-.282	2380
.19	-1.472	-.260	2070	-.281	2080	-.300	2070	-.326	2010	-.246	2260	-.267	2240	-.284	2300	-.290	2420
.20	-1.494	-.273	2120	-.292	2120	-.311	2080	-.336	2020	-.257	2320	-.277	2290	-.293	2340	-.299	2440
.22	-1.535	-.298	2170	-.315	2160	-.333	2110	-.355	2040	-.280	2390	-.297	2350	-.311	2390	-.316	2470
.24	-1.573	-.322	2200	-.338	2180	-.355	2110	-.374	2040	-.302	2430	-.316	2380	-.329	2410	-.332	2470
.26	-1.608	-.347	2200	-.360	2170	-.375	2100	-.392	2030	-.325	2440	-.336	2380	-.346	2400	-.348	2460
.28	-1.640	-.370	2190	-.381	2160	-.395	2080	-.409	2020	-.346	2430	-.354	2370	-.363	2390	-.363	2440
.30	-1.670	-.392	2160	-.401	2130	-.413	2060	-.425	2000	-.366	2390	-.372	2340	-.378	2360	-.377	2410
.32	-1.698	-.413	2130	-.420	2100	-.431	2030	-.440	1980	-.386	2360	-.388	2310	-.393	2330	-.391	2370
.34	-1.725	-.433	2090	-.438	2070	-.448	2000	-.455	1960	-.405	2310	-.404	2280	-.407	2290	-.404	2340
.36	-1.749	-.452	2050	-.456	2030	-.463	1970	-.468	1940	-.422	2260	-.420	2230	-.420	2250	-.417	2300
.38	-1.773	-.470	2000	-.472	2000	-.478	1940	-.481	1920	-.439	2210	-.434	2190	-.433	2210	-.428	2260
.40	-1.795	-.487	1960	-.487	1950	-.492	1910	-.493	1900	-.455	2170	-.448	2150	-.445	2170	-.439	2220
.42	-1.816	-.504	1920	-.502	1920	-.506	1870	-.505	1870	-.470	2110	-.461	2100	-.456	2130	-.450	2190
.44	-1.836	-.519	1880	-.516	1880	-.518	1850	-.516	1850	-.485	2070	-.473	2070	-.467	2090	-.460	2150
.46	-1.856	-.533	1840	-.529	1850	-.530	1820	-.526	1840	-.498	2020	-.485	2020	-.477	2050	-.469	2110
.48	-1.874	-.547	1800	-.541	1820	-.541	1790	-.535	1820	-.511	1980	-.496	1990	-.486	2010	-.478	2080
.50	-1.892	-.560	1760	-.553	1780	-.552	1760	-.545	1790	-.523	1930	-.506	1950	-.495	1980	-.487	2050
.55	-1.933	-.589	1680	-.579	1710	-.575	1700	-.565	1750	-.550	1840	-.530	1860	-.516	1900	-.506	1980
.60	-1.971	-.615	1610	-.602	1640	-.596	1650	-.583	1710	-.574	1750	-.551	1790	-.534	1830	-.522	1910
.65	-2.006	-.637	1550	-.622	1590	-.614	1610	-.598	1680	-.594	1690	-.569	1730	-.549	1770	-.537	1860
.70	-2.038	-.655	1500	-.639	1550	-.629	1570	-.611	1650	-.611	1630	-.584	1680	-.563	1730	-.550	1810
.75	-2.068	-.671	1460	-.653	1510	-.642	1540	-.622	1630	-.626	1580	-.598	1640	-.575	1690	-.561	1770
.80	-2.096	-.685	1420	-.666	1480	-.653	1510	-.632	1610	-.639	1540	-.609	1600	-.585	1650	-.570	1740
.85	-2.122	-.697	1390	-.676	1450	-.662	1490	-.640	1590	-.650	1510	-.619	1580	-.594	1630	-.578	1710
.90	-2.147	-.706	1370	-.685	1430	-.669	1480	-.647	1570	-.659	1490	-.628	1560	-.602	1610	-.585	1690
.95	-2.171	-.714	1350	-.692	1420	-.676	1470	-.652	1560	-.666	1470	-.635	1540	-.608	1590	-.591	1680
1.00	-2.193	-.721	1340	-.698	1410	-.681	1460	-.657	1550	-.672	1460	-.641	1530	-.614	1580	-.596	1670
1.10	-2.234	-.729	1330	-.706	1400	-.688	1460	-.664	1540	-.679	1460	-.650	1530	-.623	1580	-.604	1650
1.20	-2.272	-.733	1340	-.710	1400	-.691	1460	-.667	1540	-.683	1470	-.656	1540	-.628	1590	-.608	1650
1.30	-2.307	-.734	1350	-.711	1420	-.691	1480	-.668	1540	-.682	1500	-.658	1570	-.631	1610	-.610	1660
1.40	-2.339	-.731	1380	-.709	1440	-.689	1500	-.667	1550	-.679	1540	-.658	1610	-.632	1650	-.611	1680
1.50	-2.369	-.725	1420	-.704	1480	-.684	1540	-.664	1560	-.673	1600	-.656	1660	-.631	1700	-.609	1710
1.60	-2.397	-.717	1480	-.697	1520	-.678	1580	-.659	1580	-.665	1670	-.652	1720	-.629	1750	-.606	1750
1.70	-2.423	-.707	1530	-.689	1580	-.670	1630	-.653	1600	-.655	1750	-.646	1800	-.626	1820	-.602	1800
1.80	-2.448	-.695	1610	-.679	1640	-.661	1680	-.646	1630	-.644	1850	-.639	1880	-.621	1900	-.597	1850
1.90	-2.472	-.682	1690	-.667	1710	-.650	1750	-.638	1660	-.631	1970	-.631	1990	-.615	2000	-.591	1910
2.00	-2.494	-.667	1780	-.655	1790	-.639	1820	-.629	1690	-.616	2100	-.622	2100	-.609	2090	-.584	1980

The equations are to be used for 5.0 <= M <= 7.7 and d <= 100.0 km

Table 3. Coefficients of equations for the random and larger horizontal components of peak acceleration (in g; shear velocity in m/s).

Component	BV	VA
random	-.371	1400
larger	-.364	1390

The equations are to be used for 5.0 <= M <= 7.7 and d <= 100.0 km.

Table 4. Range of amplitudes defining the middle of the three amplitude classes used in the study of variability.

T(s)	Middle Amplitude Class (cm/s)
0.10	2.5 - 7.5
0.15	5.0 - 15.0
0.24	8.0 - 24.0
0.36	12.0 - 36.0
0.55	15.0 - 45.0
0.85	15.0 - 45.0
1.30	15.0 - 45.0
2.00	15.0 - 45.0

Table 5. Rake angles

Quake_Code	Date	Name	Rake	Reference
8	5/19/40	Imperial Valley	180	Richter (1958)
18	7/21/52	Kern County	38	Dunbar et al. (1980), Stein and Thatcher (1981)
32	3/22/57	Daly City	999	Uhrhammer (1981)
50	6/28/66	Parkfield	-160	McEvilly (1966)
58	4/09/68	Borrego Mountain	180	Allen and Nordquist (1972)
64	9/12/70	Lytle Creek	123	L. Jones, oral commun., 1993
65	2/09/71	San Fernando	76	Whitcomb (1971), Langston (1978), Heaton (1982)
76	7/30/72	Sitka	180	Schell and Ruff (1986)
79	12/23/72	Managua	0	Algermissen et al. (1974)
84	2/21/73	Point Mugu	54	Boore and Stierman (1976)
97	11/28/74	Hollister	0	Lee (1974)
137	8/13/78	Santa Barbara	57	Corbett and Johnson (1982)
144	2/28/79	St. Elias	90	Hasegawa et al. (1980) and other papers in the same issue
146	8/06/79	Coyote Lake	177	Liu and Helmberger (1983)
147	10/15/79	Imperial Valley	180	Archuleta (1984)
153	1/24/80	Livermore Valley	-159	Cockerham et al. (1980)
154	1/27/80	Livermore Valley	-176	Cockerham et al. (1980)
155	2/25/80	Horse Canyon	-169	Given (1983)
328	10/18/89	Loma Prieta	138	median of values summarized in Table 2 of Wallace et al. (1991)
349	4/25/92	Petrolia	106	Oppenheimer et al. (1993)
352	6/28/92	Landers	176	Kanamori et al. (1992)

Table 6. Coefficients for random component as a cubic function of log T for site effect in terms of site classes.

2 percent damped psv (cm/s)

COEF	C0	C1	C2	C3
B1	1.79726	2.00791	-3.74477	1.69148
B2	0.34064	-0.09703	0.34244	-0.14241
B3	-0.11823	-0.04788	0.39058	-0.23257
H	6.59550	13.59087	-40.47127	23.02134
B5	-0.95144	-0.16618	0.85766	-0.48892
B6	0.01993	0.68233	-0.58038	0.20226
B7	0.10640	0.53510	-0.01022	-0.10863
SIG1	0.20487	-0.08557	0.15702	-0.06530
SIG2	0.00650	-0.00853	0.17575	-0.07055
SIG4	0.08664	0.12758	-0.10636	0.03900

5 percent damped psv (cm/s)

COEF	C0	C1	C2	C3
B1	1.65301	1.87615	-3.17713	1.37157
B2	0.32667	-0.22536	0.64842	-0.29982
B3	-0.09803	-0.06168	0.35352	-0.20739
H	6.26923	10.59215	-32.48153	18.51690
B5	-0.93430	-0.09835	0.52386	-0.28909
B6	0.04626	0.62911	-0.57103	0.20982
B7	0.13633	0.48121	0.00514	-0.10607
SIG1	0.19117	-0.05830	0.13415	-0.05913
SIG2	0.00266	0.05649	0.07367	-0.03324
SIG4	0.08263	0.11264	-0.09145	0.03751

10 percent damped psv (cm/s)

COEF	C0	C1	C2	C3
B1	1.52871	1.64978	-2.52411	1.02345
B2	0.32446	-0.27792	0.76696	-0.36207
B3	-0.08962	-0.04338	0.29700	-0.17975
H	5.91207	7.42576	-24.29978	13.98860
B5	-0.91399	-0.03422	0.23345	-0.11598
B6	0.07422	0.53054	-0.47457	0.17644
B7	0.16035	0.44916	-0.01135	-0.08832
SIG1	0.18009	-0.03492	0.10334	-0.04458
SIG2	0.00695	0.06070	0.06191	-0.03321
SIG4	0.08368	0.07782	-0.04808	0.02375

20 percent damped psv (cm/s)

COEF	C0	C1	C2	C3
B1	1.40374	1.35854	-1.88149	0.71782
B2	0.31205	-0.17374	0.60040	-0.28394
B3	-0.08130	-0.01435	0.22199	-0.14682
H	5.66338	3.63138	-15.22173	9.13430
B5	-0.89164	-0.02480	0.08096	-0.02094
B6	0.10614	0.37912	-0.23879	0.05560
B7	0.19135	0.37854	0.05437	-0.12154
SIG1	0.16865	0.00125	0.04311	-0.01424
SIG2	0.02248	0.00721	0.13665	-0.07236
SIG4	0.08637	0.06515	-0.05932	0.03907

Table 7. Coefficients for larger component as a cubic function of log T for site effect in terms of site classes.

2 percent damped psv (cm/s)

COEF	C0	C1	C2	C3
B1	1.85796	2.10449	-3.86361	1.78453
B2	0.33735	0.02393	0.09652	-0.01644
B3	-0.12183	-0.10318	0.44112	-0.23046
H	6.47604	13.98567	-41.57274	23.87958
B5	-0.95121	-0.23530	1.04519	-0.63494
B6	0.01260	0.68300	-0.59046	0.21780
B7	0.10115	0.53786	-0.06125	-0.06862
SIG1	0.20725	-0.03834	0.08832	-0.03828
SIG2	-0.00940	0.10622	-0.04323	0.05615
SIG4	0.00000	0.00000	0.00000	0.00000

5 percent damped psv (cm/s)

COEF	C0	C1	C2	C3
B1	1.70003	1.97979	-3.22270	1.40062
B2	0.32059	-0.02727	0.24853	-0.09759
B3	-0.10401	-0.15801	0.51107	-0.26515
H	6.18210	10.61936	-33.14299	19.21283
B5	-0.92131	-0.22383	0.76539	-0.44561
B6	0.03851	0.67250	-0.71115	0.30472
B7	0.12763	0.54306	-0.20159	0.02785
SIG1	0.19415	-0.01519	0.07312	-0.03526
SIG2	-0.01134	0.11701	-0.05236	0.05945
SIG4	0.00000	0.00000	0.00000	0.00000

10 percent damped psv (cm/s)

COEF	C0	C1	C2	C3
B1	1.56253	1.71556	-2.43821	0.97456
B2	0.32384	-0.06350	0.34072	-0.15288
B3	-0.10648	-0.10248	0.40387	-0.21639
H	5.59958	7.90340	-25.16582	14.63759
B5	-0.88607	-0.20312	0.49729	-0.26520
B6	0.06747	0.60771	-0.69866	0.31415
B7	0.14209	0.58968	-0.35920	0.11128
SIG1	0.18659	-0.02435	0.09240	-0.04125
SIG2	-0.00998	0.08911	0.00870	0.02598
SIG4	0.00000	0.00000	0.00000	0.00000

20 percent damped psv (cm/s)

COEF	C0	C1	C2	C3
B1	1.44367	1.41124	-1.81388	0.69053
B2	0.32379	0.04440	0.13760	-0.05847
B3	-0.10169	-0.06309	0.31892	-0.17940
H	5.43053	4.06257	-16.03367	9.71543
B5	-0.87365	-0.15375	0.29499	-0.14823
B6	0.10701	0.37611	-0.31027	0.11562
B7	0.17728	0.43727	-0.12623	-0.00918
SIG1	0.17835	-0.02316	0.08933	-0.03507
SIG2	0.00122	0.02929	0.13472	-0.05018
SIG4	0.00000	0.00000	0.00000	0.00000

Table 8. Coefficients for random component as a cubic function of log T for site effect in terms of continuous shear velocity.

2 percent damped psv (cm/s)

COEF	C0	C1	C2	C3
B1	1.79726	2.00791	-3.74477	1.69148
B2	0.34064	-0.09703	0.34244	-0.14241
B3	-0.11823	-0.04788	0.39058	-0.23257
H	6.59550	13.59087	-40.47127	23.02134
B5	-0.95144	-0.16618	0.85766	-0.48892
BV	-0.19059	0.11211	-1.55398	0.91181
LOGVA	2.98711	2.03539	-3.51026	1.61535
SIG1	0.20487	-0.08557	0.15702	-0.06530
SIG2	0.00650	-0.00853	0.17575	-0.07055
SIG4	0.08664	0.12758	-0.10636	0.03900

5 percent damped psv (cm/s)

COEF	C0	C1	C2	C3
B1	1.65301	1.87615	-3.17713	1.37157
B2	0.32667	-0.22536	0.64842	-0.29982
B3	-0.09803	-0.06168	0.35352	-0.20739
H	6.26923	10.59215	-32.48153	18.51690
B5	-0.93430	-0.09835	0.52386	-0.28909
BV	-0.21172	0.06619	-1.35085	0.79809
LOGVA	3.04586	1.69975	-2.97445	1.37668
SIG1	0.19117	-0.05830	0.13415	-0.05913
SIG2	0.00266	0.05649	0.07367	-0.03324
SIG4	0.08263	0.11264	-0.09145	0.03751

10 percent damped psv (cm/s)

COEF	C0	C1	C2	C3
B1	1.52871	1.64978	-2.52411	1.02345
B2	0.32446	-0.27792	0.76696	-0.36207
B3	-0.08962	-0.04338	0.29700	-0.17975
H	5.91207	7.42576	-24.29978	13.98860
B5	-0.91399	-0.03422	0.23345	-0.11598
BV	-0.22228	-0.01615	-1.13584	0.69342
LOGVA	3.11715	1.27112	-2.32329	1.09915
SIG1	0.18009	-0.03492	0.10334	-0.04458
SIG2	0.00695	0.06070	0.06191	-0.03321
SIG4	0.08368	0.07782	-0.04808	0.02375

20 percent damped psv (cm/s)

COEF	C0	C1	C2	C3
B1	1.40374	1.35854	-1.88149	0.71782
B2	0.31205	-0.17374	0.60040	-0.28394
B3	-0.08130	-0.01435	0.22199	-0.14682
H	5.66338	3.63138	-15.22173	9.13430
B5	-0.89164	-0.02480	0.08096	-0.02094
BV	-0.25076	-0.06079	-0.90611	0.56054
LOGVA	3.17909	0.79899	-1.45838	0.67158
SIG1	0.16865	0.00125	0.04311	-0.01424
SIG2	0.02248	0.00721	0.13665	-0.07236
SIG4	0.08637	0.06515	-0.05932	0.03907

Table 9. Coefficients for larger component as a cubic function of log T for site effect in terms of continuous shear velocity.

2 percent damped psv (cm/s)

COEF	C0	C1	C2	C3
B1	1.85796	2.10449	-3.86361	1.78453
B2	0.33735	0.02393	0.09652	-0.01644
B3	-0.12183	-0.10318	0.44112	-0.23046
H	6.47604	13.98567	-41.57274	23.87958
B5	-0.95121	-0.23530	1.04519	-0.63494
BV	-0.18756	0.14232	-1.50203	0.87573
LOGVA	2.97650	2.32001	-3.96875	1.83679
SIG1	0.20725	-0.03834	0.08832	-0.03828
SIG2	-0.00940	0.10622	-0.04323	0.05615
SIG4	0.00000	0.00000	0.00000	0.00000

5 percent damped psv (cm/s)

COEF	C0	C1	C2	C3
B1	1.70003	1.97979	-3.22270	1.40062
B2	0.32059	-0.02727	0.24853	-0.09759
B3	-0.10401	-0.15801	0.51107	-0.26515
H	6.18210	10.61936	-33.14299	19.21283
B5	-0.92131	-0.22383	0.76539	-0.44561
BV	-0.20688	0.05736	-1.16511	0.67327
LOGVA	3.03221	1.96183	-3.37489	1.56641
SIG1	0.19415	-0.01519	0.07312	-0.03526
SIG2	-0.01134	0.11701	-0.05236	0.05945
SIG4	0.00000	0.00000	0.00000	0.00000

10 percent damped psv (cm/s)

COEF	C0	C1	C2	C3
B1	1.56253	1.71556	-2.43821	0.97456
B2	0.32384	-0.06350	0.34072	-0.15288
B3	-0.10648	-0.10248	0.40387	-0.21639
H	5.59958	7.90340	-25.16582	14.63759
B5	-0.88607	-0.20312	0.49729	-0.26520
BV	-0.21500	-0.04212	-0.87726	0.52041
LOGVA	3.08843	1.70863	-2.99685	1.39965
SIG1	0.18659	-0.02435	0.09240	-0.04125
SIG2	-0.00998	0.08911	0.00870	0.02598
SIG4	0.00000	0.00000	0.00000	0.00000

20 percent damped psv (cm/s)

COEF	C0	C1	C2	C3
B1	1.44367	1.41124	-1.81388	0.69053
B2	0.32379	0.04440	0.13760	-0.05847
B3	-0.10169	-0.06309	0.31892	-0.17940
H	5.43053	4.06257	-16.03367	9.71543
B5	-0.87365	-0.15375	0.29499	-0.14823
BV	-0.23244	-0.00352	-0.87542	0.51529
LOGVA	3.18688	1.25622	-2.28521	1.06378
SIG1	0.17835	-0.02316	0.08933	-0.03507
SIG2	0.00122	0.02929	0.13472	-0.05018
SIG4	0.00000	0.00000	0.00000	0.00000

Table 10. Changes in Site Classification

Sta_Code	Name	G(old)	G(new)
455	Capitola	B	C
498	Halls Valley	B	C
496	SAGO South	A	B
458	San Francisco: Diamond Heights	A	B

Table 11: Borehole Information (AvgVel in m/s).

HOLE#	SITE NAME	LAT.	LONG.	AVGVEL	COMMENTS	REFERENCE
209	Monterey	36.597	121.897	763	extrpltd 10.49m to 30 m (based on El Granada, OFR 75-564).	Thiel and Schneider (1993)
210	Belmont	37.512	122.308	628	no tt extrapolation	Thiel and Schneider (1993)
211	Sago South (Hollister Hills)	36.753	121.396	612	extrapolated 10.49m to 30m (needs 6993 m/s to reach 750 m/s).	Thiel and Schneider (1993)
212	Piedmont Jr. High School	37.823	122.233	896	extrpltd 2m to 30m	Thiel and Schneider (1993)
213	San Francisco, Rincon Hill	37.786	122.391	872	extrpltd 5.9 m to 30 m.	Thiel and Schneider (1993)
214	San Francisco, Pacific Heights	37.790	122.429	1250	no tt extrapolation	Thiel and Schneider (1993)
215	Lexington Dam	37.202	121.949	1071	tt extrpltd 7.51m to 30m	Thiel and Schneider (1993)
216	San Francisco, Diamond Heights	37.740	122.433	584	extrapolated 0.1 m to 30 m.	Thiel and Schneider (1993)
217	Point Bonita	37.820	122.520	1316	tt extrapolated 0.1 m to 30 m.	Thiel and Schneider (1993)
218	Berkeley, Haviland Hall	37.870	122.260	1266	no tt extrapolation (but used suspension logging results)	Thiel and Schneider (1993)
219	Capitola	36.974	121.952	289	no tt extrapolation	Thiel and Schneider (1993)
220	So. San Francisco, Sierra Poin	37.674	122.388	1020	tt extrapolated 2.81 m to 30 m.	Thiel and Schneider (1993)
221	Agnews Hospital	37.397	121.952	264	no tt extrapolation	Thiel and Schneider (1993)
222	Livermore, Patterson Pass	37.702	121.684	377	tt extrapolated 0.1 m to 30 m.	Thiel and Schneider (1993)
223	Martinez V. A. Hospital	37.993	122.115	384	no tt extrapolation	Thiel and Schneider (1993)
224	Mission San Jose	37.530	121.919	368	no tt extrapolation	Thiel and Schneider (1993)
225	Santa Cruz	37.001	122.060		no subsurface geophysics, shallow hole with voids	Thiel and Schneider (1993)
226	Richmond City	37.935	122.342	260	no tt extrapolation	Thiel and Schneider (1993)
227	Menlo Park V. A. Hospital	37.468	122.157	267	no tt extrapolation	Thiel and Schneider (1993)
229	San Francisco VA Medical Cente	37.783	122.504	550	no tt extrapolation	Thiel and Schneider (1993)
230	Halls Valley - Grant Park	37.338	121.714	265	no tt extrapolation	Thiel and Schneider (1993)
231	UC Berkeley Memorial Stadium	37.870	122.250	472	no tt extrapolation	Thiel and Schneider (1993)
232	Oakland Two Story	37.806	122.267	323	velocity based on suspension log; CUREE hole closer to sm than USG	Thiel and Schneider (1993)
233	Lawrence Livermore, Site 300			685	coordinates not given in CUREE report; LLNL recorded LP89 here.	Thiel and Schneider (1993)

Note: AVGVEL = 30m divided by the travel time to 30m; units are m/s.

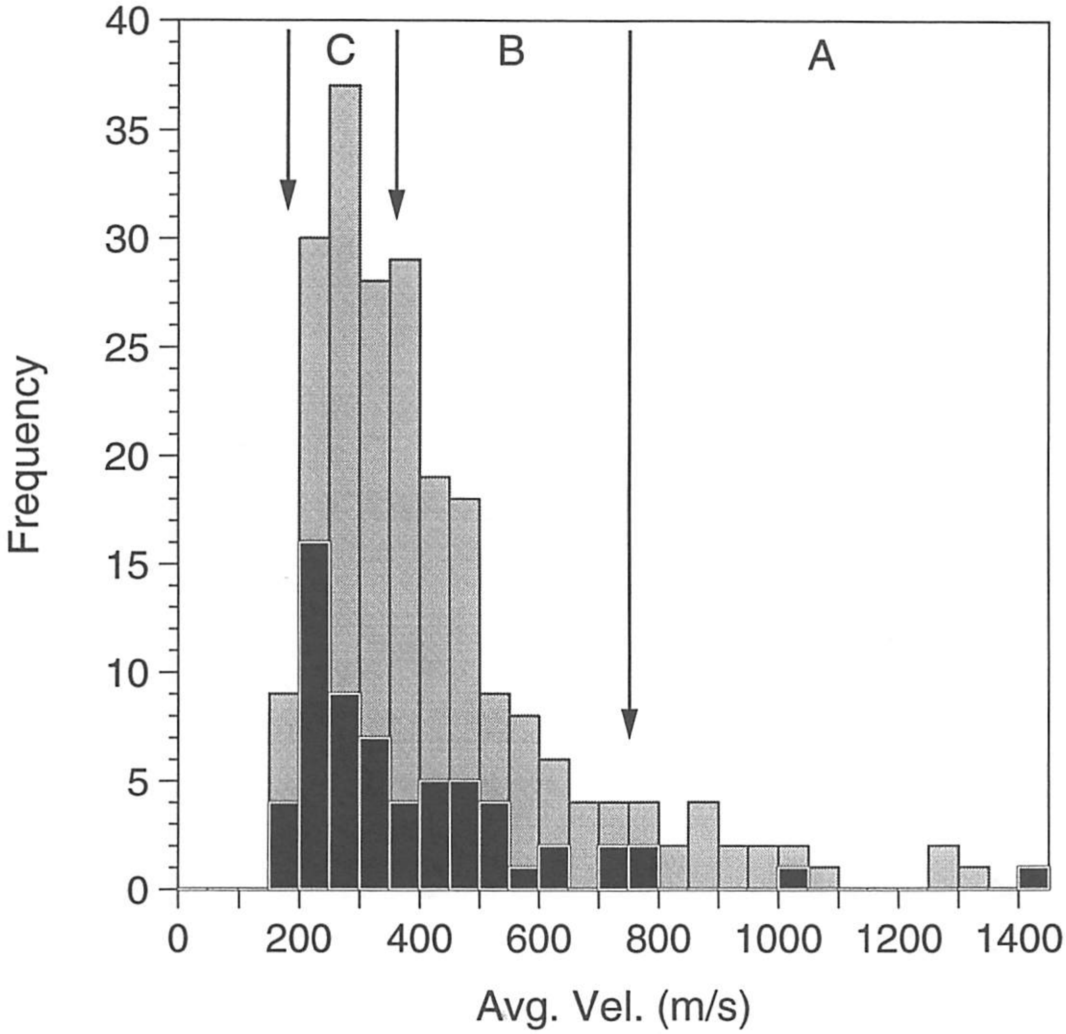

Figure 1. Histogram of average velocities, with boundaries between site classes shown by the arrows. The black bars are for those sites used in the regression analysis to determine the velocity dependence of response spectra, and the gray bars represent the distribution of the published shear-velocity data. It should be noted that the distribution shown by the gray bars does not necessarily represent the distribution that would be obtained for the shear-wave velocities from the population of strong-motion stations.

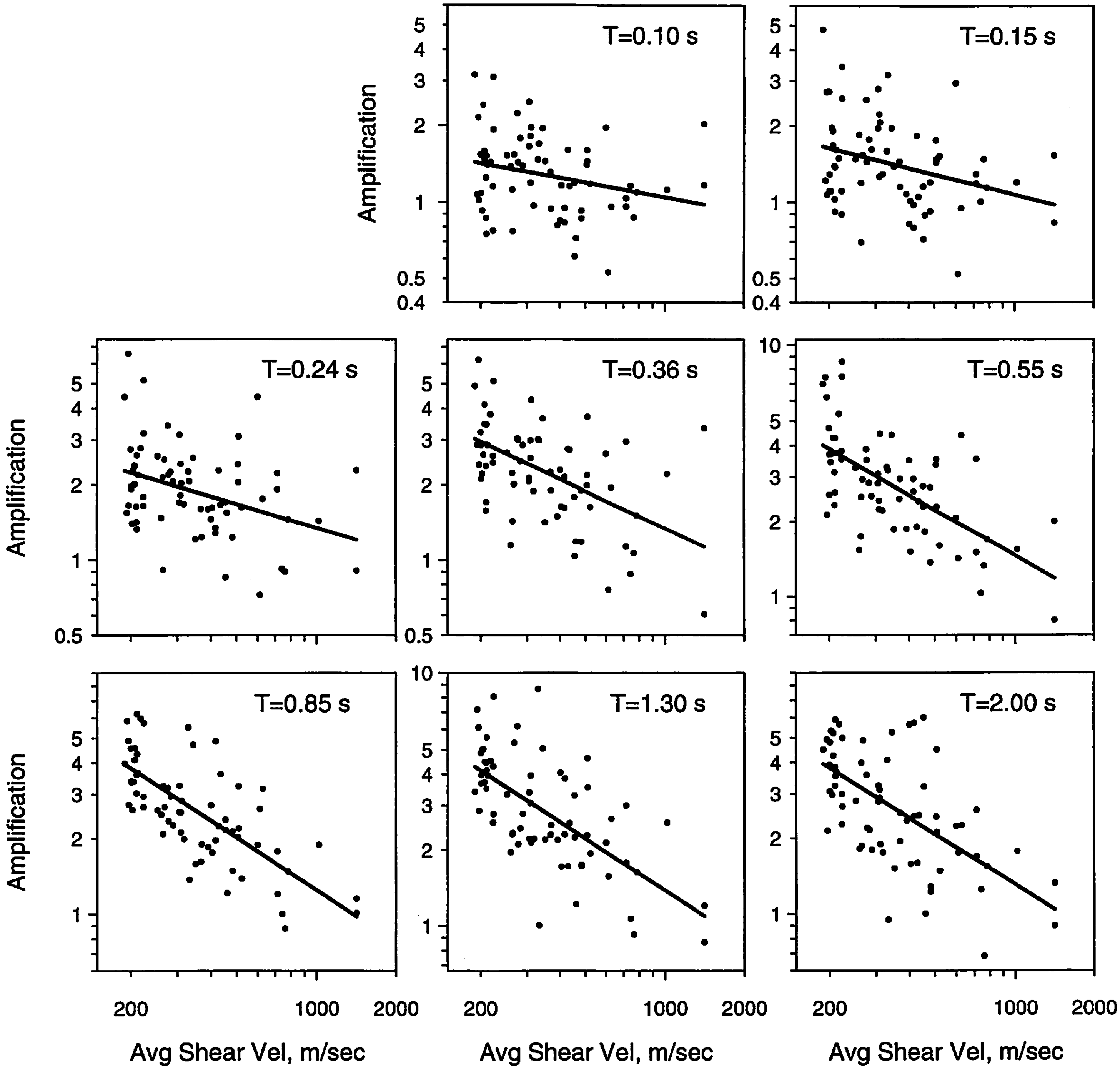

Figure 2. Amplification of 5 percent-damped response spectra for the random component as a function of average shear velocity, as given by equation (3). T is the oscillator period, in seconds. The dots are the data used to determine the velocity dependence.

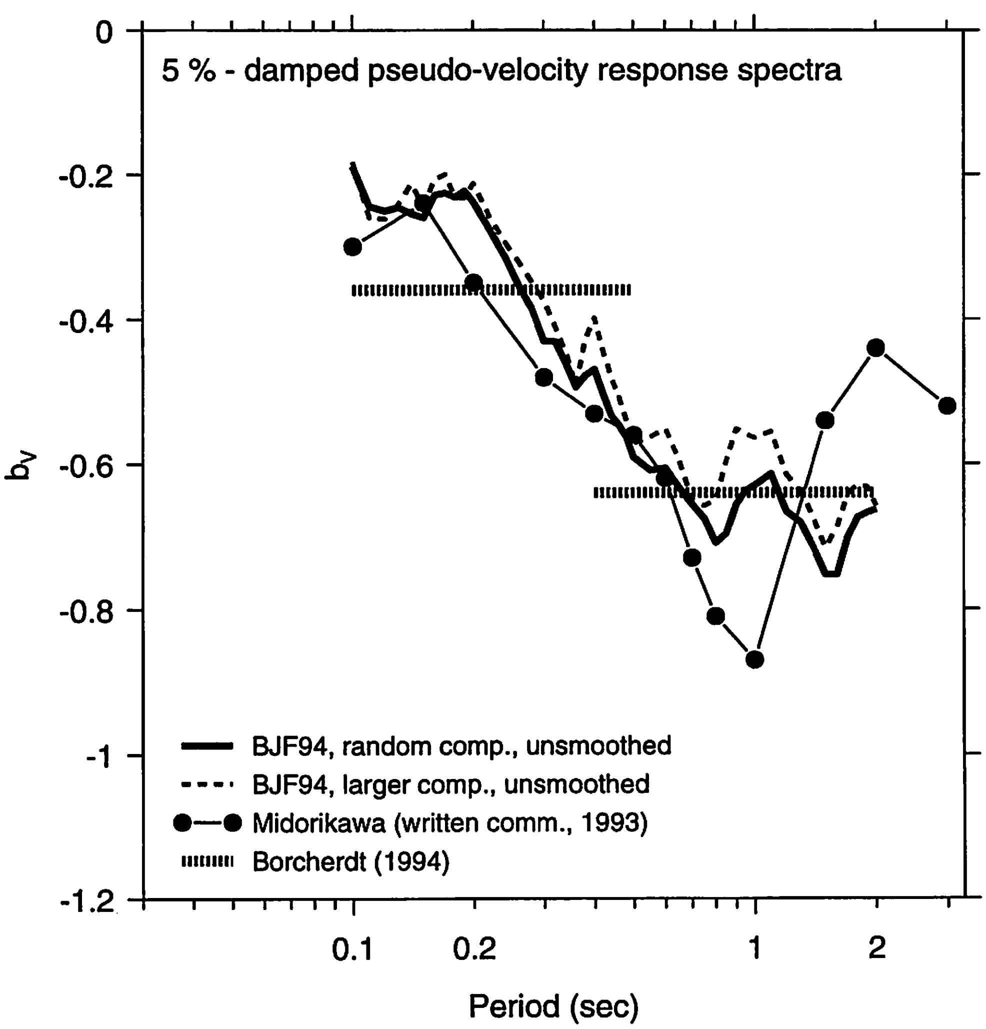

Figure 3. The coefficient that controls the shear-velocity dependence of response spectral amplification, as determined in this study for California data and by Midorikawa (written communication, 1993) for data from Japan. Also shown are the coefficients proposed by Borcherdt (1994) for determining short-period and mid-period amplification factors in building codes; these were determined from Fourier amplitude spectra of recordings from the Loma Prieta earthquake.

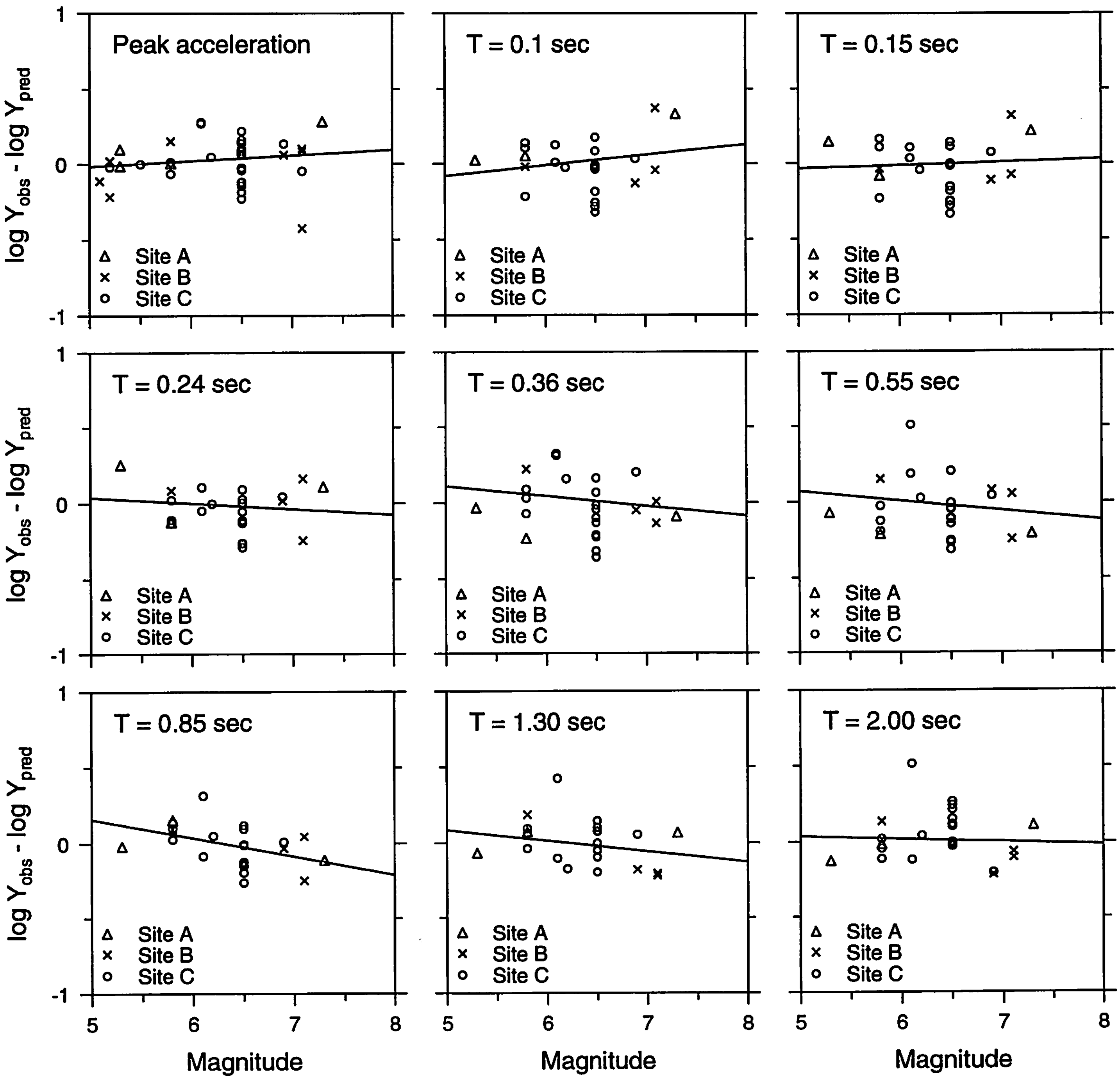

Figure 4. Residuals of peak acceleration and 5 percent-damped response spectra for the random component at distances less than 10 km, with straight line fit to the residuals. T is the oscillator period, in seconds. The only slope that is significantly different than zero is that for the 0.85 sec oscillator.

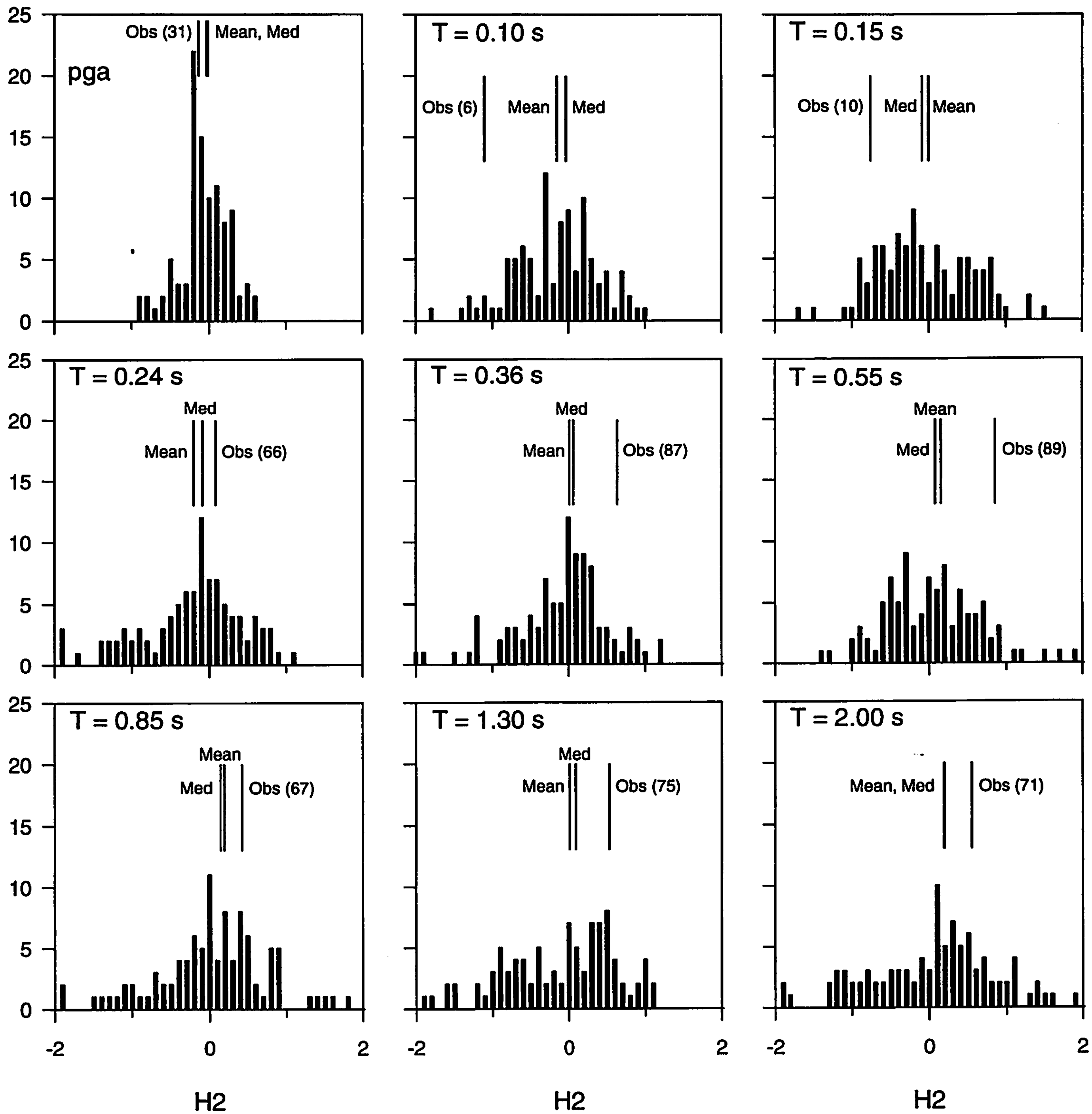

Figure 5. Histograms of h_2 determined from regression analyses of 100 simulated data sets obtained by setting $h_2 = 0$, for peak acceleration and 5 percent-damped response spectra, random component. T is the oscillator period, in seconds. The lines show the mean and median values of h_2 from the simulated data, as well as the value of h_2 obtained from analysis of the observed data. The number in parenthesis after "Obs" is the percentage of h_2's from the simulated data that fall below the value obtained from the observed data.

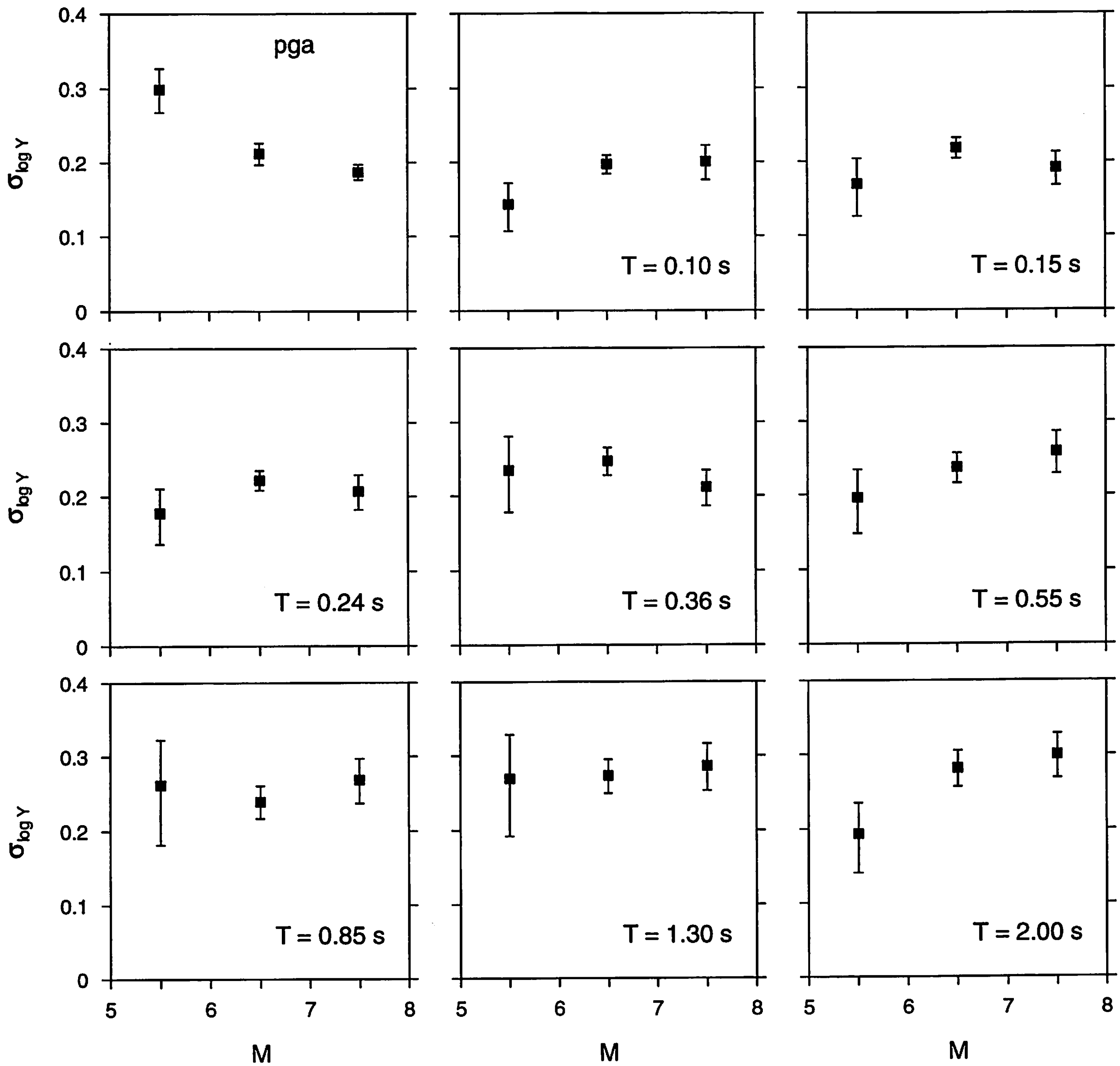

Figure 6. $\sigma_{\log Y}$ as a function of M, for peak acceleration and 5 percent-damped response spectra, random component. T is the oscillator period, in seconds.

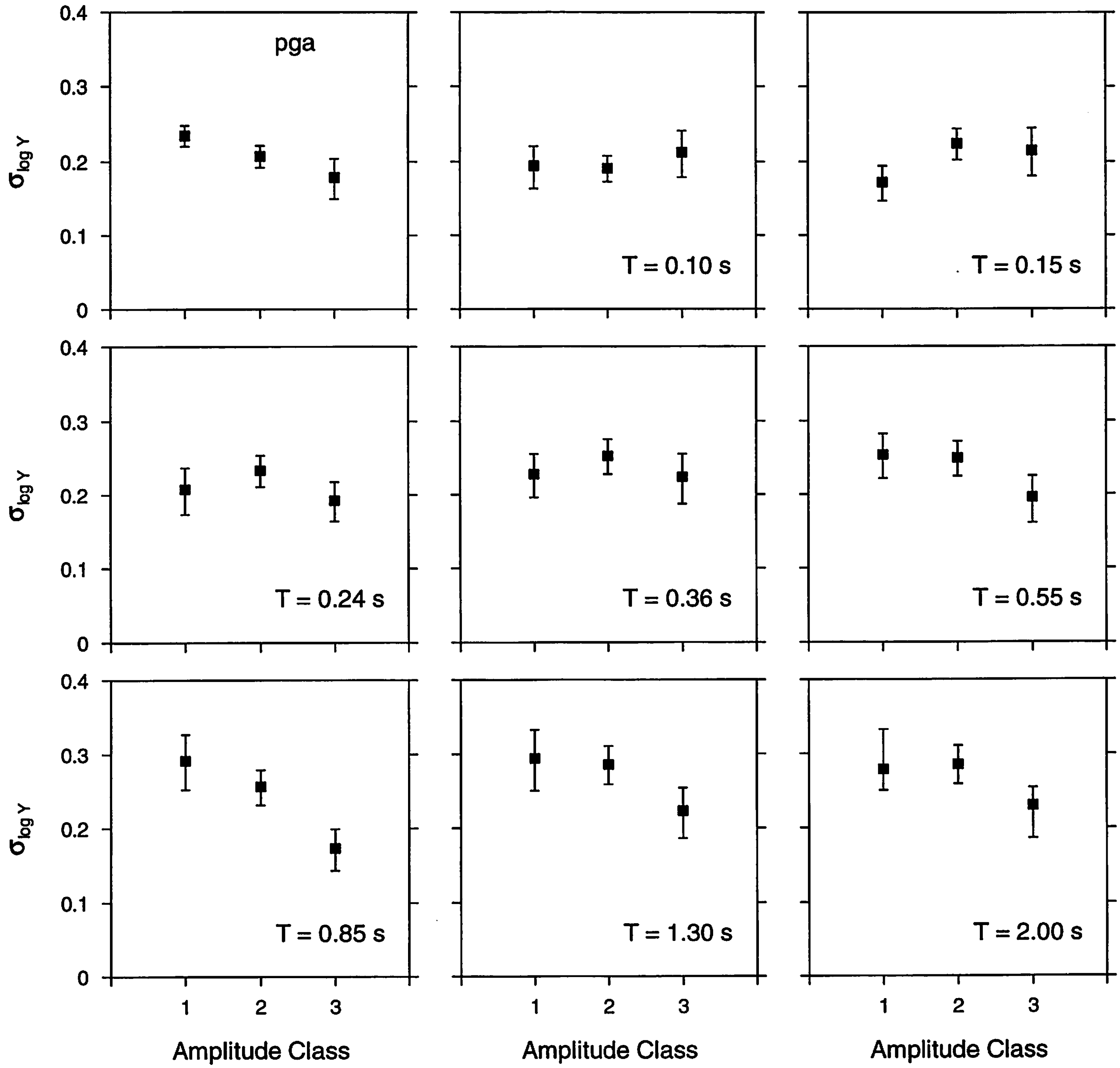

Figure 7. $\sigma_{\log Y}$ as a function of amplitude class, for peak acceleration and 5 percent-damped response spectra, random component. T is the oscillator period, in seconds.

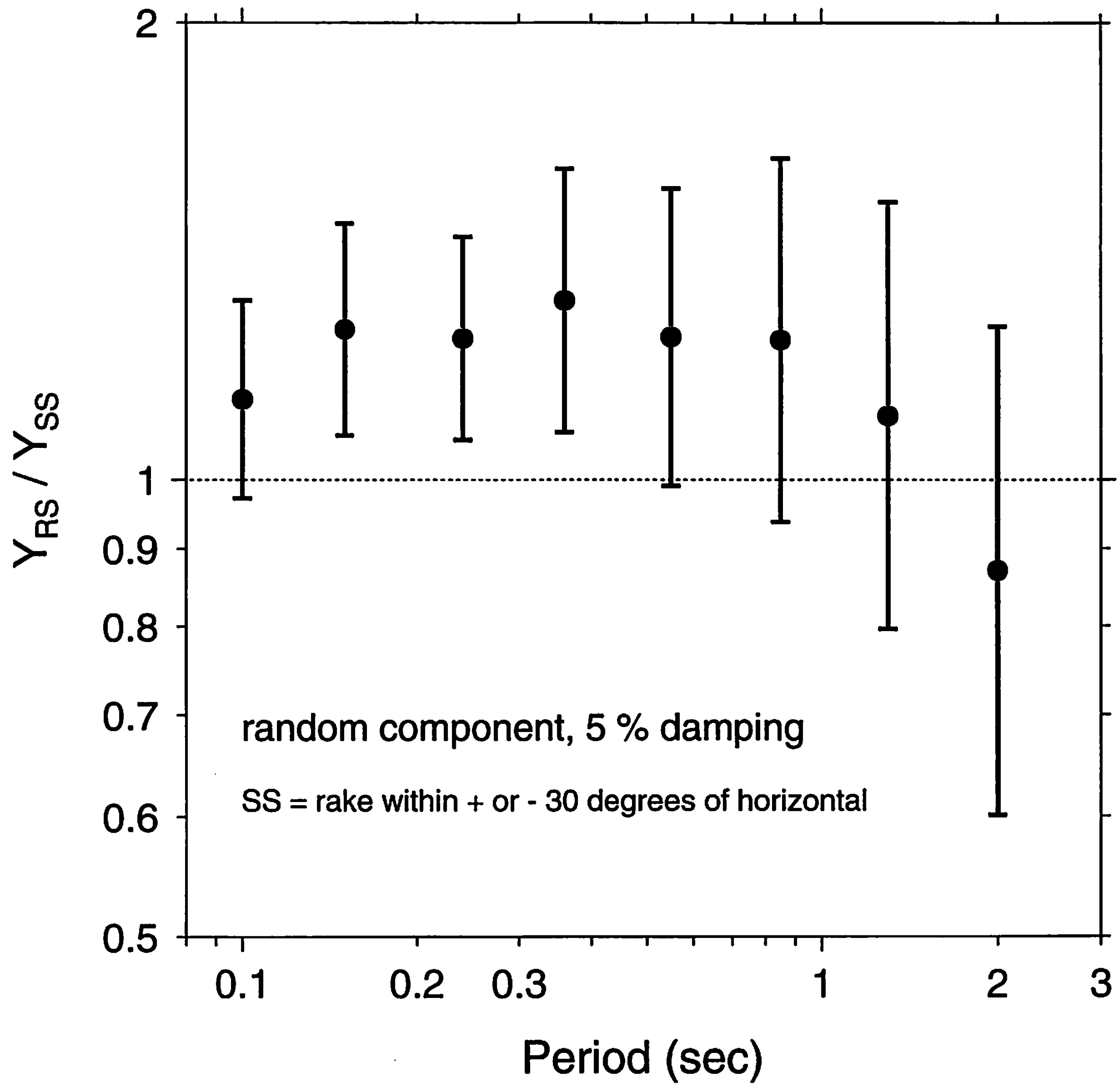

Figure 8. Ratio of response spectral values between reverse-slip and strike-slip earthquakes, as a function of oscillator period.

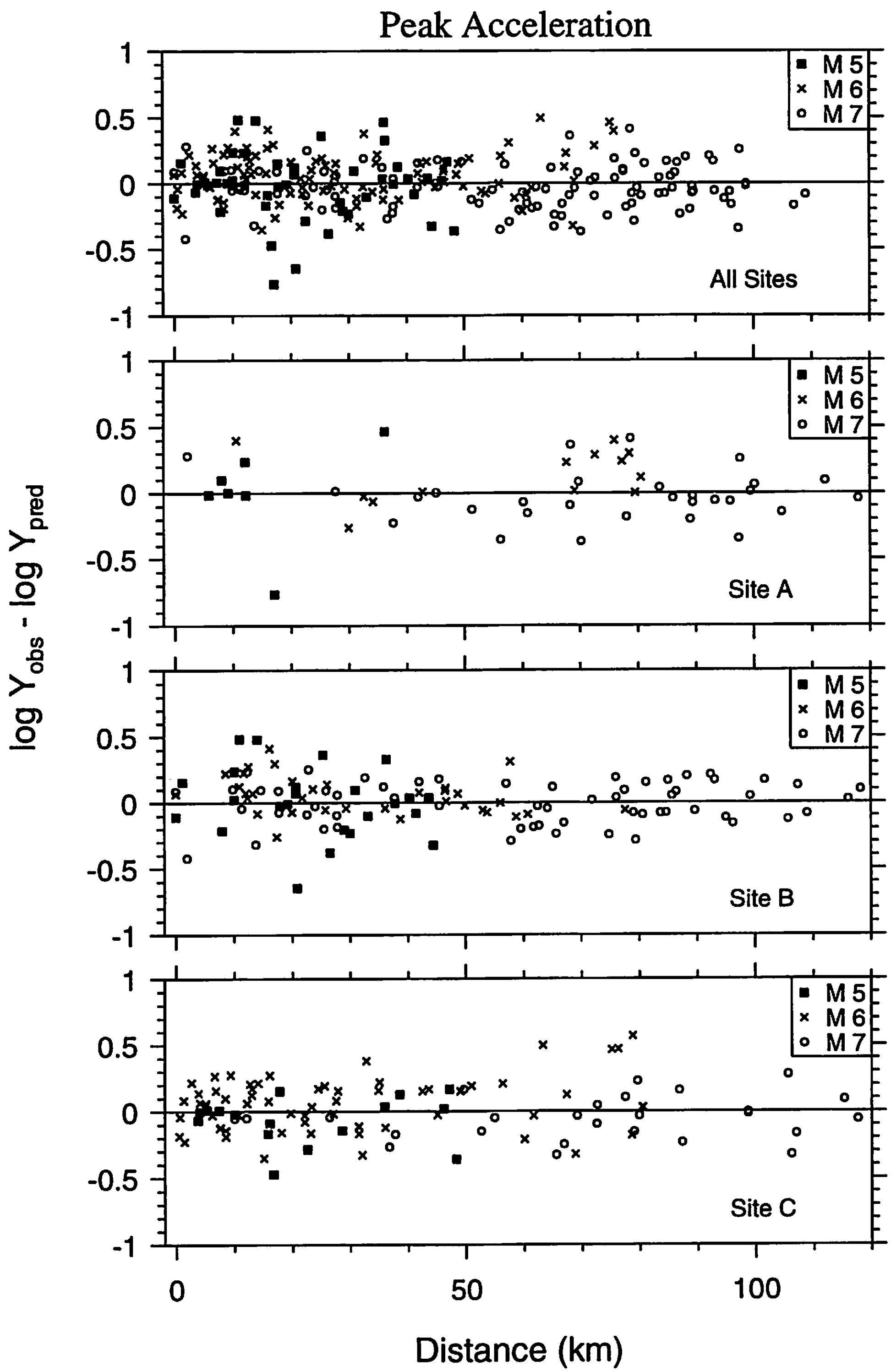

Figure 9. Residuals for peak acceleration.

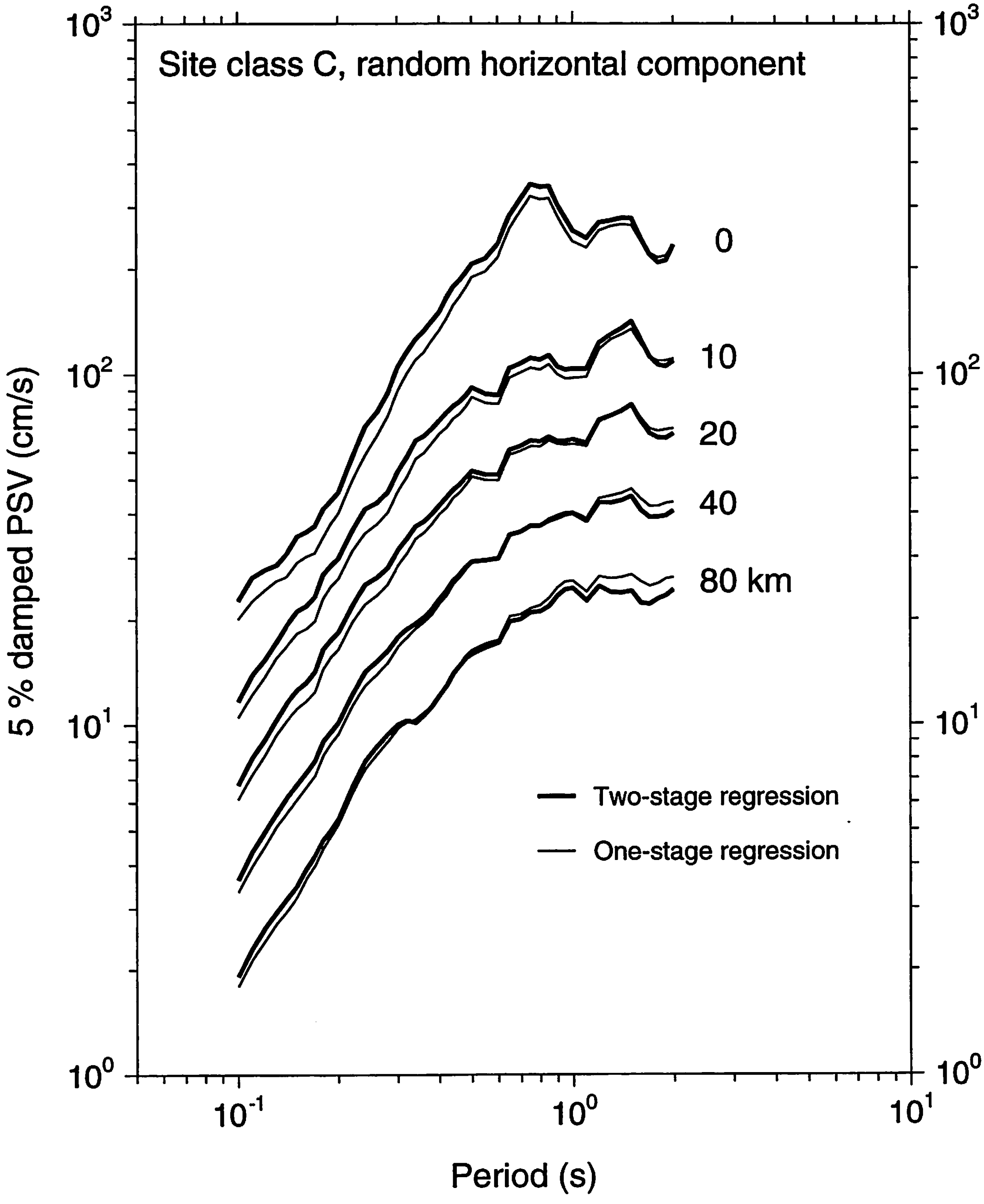

Figure 10. Comparison of one and two-stage regressions.